



3 4456 0382489 6

ORNL/TM-7438/V2

ornl

**OAK
RIDGE
NATIONAL
LABORATORY**



Ocean Thermal Energy Conversion Gas Desorption Studies

Vol. 2. Deaeration in a Packed Column
and a Barometric Intake System

A. Golshani
F. C. Chen

OAK RIDGE NATIONAL LABORATORY

CENTRAL RESEARCH LIBRARY

CIRCULATION SECTION

4500N ROOM 175

LIBRARY LOAN COPY

DO NOT TRANSFER TO ANOTHER PERSON

If you wish someone else to see this
report, send in name with report and
the library will arrange a loan.

UCN-7969 (3 9-77)

OPERATED BY
UNION CARBIDE CORPORATION
FOR THE UNITED STATES
DEPARTMENT OF ENERGY

Contract No. W-7405-eng-26

OCEAN THERMAL ENERGY CONVERSION GAS DESORPTION STUDIES

Vol. 2. Deaeration in a Packed Column
and a Barometric Intake System

A. Golshani
Engineering Technology Division

F. C. Chen
Energy Division

Date Published: September 1981

NOTICE This document contains information of a preliminary nature.
It is subject to revision or correction and therefore does not represent a
final report.

Prepared for the
Department of Energy
Ocean Energy Systems Division

Prepared by the
OAK RIDGE NATIONAL LABORATORY
Oak Ridge, Tennessee 37830
operated by
UNION CARBIDE CORPORATION
for the
DEPARTMENT OF ENERGY



3 4456 0382489 6



CONTENTS

	<u>Page</u>
ACKNOWLEDGMENTS	v
NOMENCLATURE	vii
ABSTRACT	1
1. INTRODUCTION	1
2. BACKGROUND	3
3. TEST LOOP DESIGN	7
3.1 Modification of Dissolved Oxygen Measurement	7
3.2 Description of Equipment	7
3.3 General Flow Description	10
3.4 Test Section Packed Column	11
3.5 Flow Control Water Pumps	13
3.6 Oxygen-Measuring Station	13
3.7 Vacuum System	13
3.8 Barometric-Leg Water Holding Tank	14
3.9 Barometric Intake System	14
3.10 Steady-State Operation	15
4. RESULTS AND DISCUSSION	16
4.1 Results of Vacuum Deaeration in a Packed Column	16
4.2 Correlation of Data	29
4.3 Maximum Flow of Water Through Packed Column	32
4.4 Results of Deaeration in the Barometric Leg of the Intake System	32
4.5 Application to OTEC Open-Cycle Plant and Economic Evaluation	47
5. CONCLUSIONS	50
REFERENCES	51
APPENDIX. ESTIMATED VALUE OF HTU FOR 8.89-cm (3.5-in.) PLASTIC PALL RING	53

•

•

•

•

•

•

ACKNOWLEDGMENTS

This investigation was performed at the Oak Ridge National Laboratory (ORNL), operated by Union Carbide Corporation for the Department of Energy (DOE). The study was a part of the general Ocean Energy Conversion program being carried out by ORNL for the DOE Ocean Energy Systems Division.

The authors wish to express their appreciation for the assistance of many ORNL staff members, particularly H. W. Hoffman, J. W. Michel, and R. W. Murphy for their helpful suggestions throughout the program and R. L. Linkous (project technician) for operating the test equipment, collecting data, and writing Sect. 3 (Test Loop Design) of this report.

•

•

•

•

•

•

NOMENCLATURE

a	effective area of liquid gas interface per unit volume, m^2/m^3
d	diameter of packed column, cm
D	coefficient of diffusion for solute gas in liquid, m^2/h
h	total height of deaerator, cm
H	Henry's law constant, $\frac{(kg \text{ mole}/m^3)}{kPa}$
h_1	height of packing [(NTU)•(HTU)], cm
h_{end}	height of packing equivalent to end effects, cm
HTU	height of transfer unit (using liquid), cm
k_{ga}	gas film coefficient, $\frac{kg \text{ mole}}{(h \cdot m^3)(kg \text{ mole}/m^3)}$
K_{La}	overall coefficient based on concentration
k_{La}	liquid film coefficient, $\frac{kg \text{ mole}}{(h \cdot m^3)(kg \text{ mole}/m^3)}$
L	liquid flow rate, $kg/(h \cdot m^2)$
L_{max}	maximum liquid flow rate for a given packing, $kg/(h \cdot m^2)$
M	molecular weight
NPD	normalized percentage of deaeration, $(X_i - X_o)/(X_i - X_e)$
NTU	number of transfer units
p	pressure of gas in the gas phase, kPa
P_{air}	absolute vacuum air pressure, kPa
PDA	percentage of deaeration, $(X_i - X_o)/X_i$
QL	liquid flow rate, m^3/h
Re	Reynolds number
S	empirical constant
Sc	Schmidt number
v	water velocity, cm/s
W_{hsw}	warm seawater flow, kg/h
X_I	concentration of solute in liquid entering tower, $\frac{kg \text{ gas}}{kg \text{ water}} \times 10^6$, ppm

x_0	concentration of solute in liquid leaving tower, $\frac{\text{kg gas}}{\text{kg water}} \times 10^6$, ppm
x_e	concentration of solute in liquid in equilibrium with gas phase
x	cost of packing support plate, $\$/\text{m}^2$
y	cost of liquid distributors, $\$/\text{m}^2$
z	cost of packing, $\$/\text{m}^3$
α	empirical constant
ϵ	stage efficiency
η	overall deaerator efficiency
μ	viscosity, $\text{Pa}\cdot\text{s}$
ρ	density, kg/m^3

OCEAN THERMAL ENERGY CONVERSION GAS DESORPTION STUDIES

Vol. 2. Deaeration in a Packed Column and a Barometric Intake System

A. Golshani F. C. Chen

ABSTRACT

Seawater deaeration is a process affecting almost all proposed Ocean Thermal Energy Conversion (OTEC) open-cycle power systems. If the noncondensable dissolved air is not removed from a power system, it will accumulate in the condenser, reduce the effectiveness of condensation, and result in deterioration of system performance. A gas desorption study was initiated at Oak Ridge National Laboratory (ORNL) to mitigate these effects; this study is designed to investigate the vacuum deaeration process for OTEC conditions where conventional steam-stripping deaeration may not be applicable. Studies were carried out in two areas: (1) vacuum deaeration in a packed column and (2) deaeration in a barometric intake system.

As the second in a series describing the ORNL studies, this report (1) reviews previous relevant studies, (2) describes the design of a gas desorption test loop and a barometric intake system, (3) presents the results of vacuum deaeration in a packed column and a barometric intake system, and (4) discusses the savings that can be achieved when the packed column is combined with the barometric intake system.

Vacuum deaeration laboratory experiments using three different kinds of packings in a packed column test section and a series of barometric intake deaeration experiments have been performed. A conceptual OTEC deaeration subsystem design, based on these results, and its implications on an OTEC-open cycle power system are presented.

1. INTRODUCTION

Deaeration (noncondensibles removal) is a gas desorption process. Since the major power components of Ocean Thermal Energy Conversion (OTEC) open-cycles (including Claude- and various lift-cycle concepts) will be operating under a subatmospheric pressure environment, deaeration and/or noncondensibles removal from the power systems are essential to maintain the proper power generation efficiency.

A gas desorption study was initiated, and a test loop was assembled to investigate various concepts of vacuum deaeration and noncondensibles removal. The previous activities of the Oak Ridge National Laboratory (ORNL) study¹ included (1) theories of gas desorption, (2) design of experiments, (3) previous relevant studies, (4) description of the gas desorption test plan, and (5) preliminary test results and discussions.

In the present report, results of additional packed column tests on different kinds of packings are presented, and the deaeration test of a barometric intake system is discussed. In the Claude-cycle OTEC power system, warm seawater at ambient pressure is fed to a vacuum flash evaporator through a barometric intake system. The hydrostatic pressure of water gradually decreases in the barometric intake pipe as warm seawater flows upward. Dissolved air in seawater will be evolved under these conditions. Claude had included the barometric intake deaeration concept in his design of an OTEC open-cycle power system.² Deaeration in a barometric intake pipe is affected by physical and geometrical parameters such as system pressure drop, mass flow, friction, pipe diameter, and existing nuclei in seawater. A literature search indicated no previous investigation on this subject. Barometric-leg deaeration should have the advantage of partial predeaeration and thus avoid part of the cost penalty of adding an extra component; a systematic study of the concept was initiated.

This report documents the deaeration experiments on packed columns and the barometric intake system. Results derived from these tests are used to update the conceptual baseline design of the deaeration subsystem of the 100-MWe open-cycle power system.

2. BACKGROUND

Gas desorption from water is a mass-transfer phenomenon. Like any transfer process, the movement of dissolved gas in the liquid phase is driven by the overall available concentration gradient across the interphase and is retarded by diffusional and interfacial resistances in and between the phases. The rate of gas desorption in a device can be increased for given concentration-gradient differences either by reducing the diffusional and interfacial resistances or by increasing the available surface area. Falling film configuration is an example of a gas desorption device in which a high mass-transfer coefficient is maintained by reducing the liquid film thickness. Steam or foreign-gas stripping is usually used in gas desorption operations to maintain a high overall partial-pressure difference when the column is operated at higher total pressure. Increasing the flow turbulence level by dynamic agitation or by static turbulent promoters can reduce diffusional and interfacial resistances. The use of packing increases the interfacial area.

The mass-transfer coefficient k_L is proportional to the molecular diffusion coefficient D in the stagnant film theory and is proportional to the square root of D in the penetration and surface-renewal theories.³⁻⁵ Among the other theories, k_L was correlated with D to the n th power for values of n lying between 0.50 and 0.75, depending on the fluid dynamic conditions of the experiments.

The performance of a gas desorption device may involve two or more means of maintaining a high concentration gradient: (1) steam stripping and/or (2) reducing diffusional resistance and extending interphase area by using packed columns and spray towers. However, the combination of these effects and the complicated geometry make theoretical analysis difficult. In Sherwood and Holloway's study⁶ of gas desorption in a packed column and in many later similar studies, simple theoretical models were unable to predict the gas desorption phenomenon. Concepts of liquid and gas film coefficients (k_{La} , k_{ga}), height of transfer units (HTU), and number of transfer units (NTU) were introduced and used to correlate gas desorption data empirically with various nondimensional parameters.

A modified version of the empirical correlation formula proposed by Sherwood and Holloway² is commonly used in gas desorption studies:

$$k_L a/D = \alpha(L/\mu)^{1-n}(\mu/\rho D)^{1-s} , \quad (1)$$

and

$$(\text{HTU})_L = 1/\alpha(L/\mu)^n(\mu/\rho D)^s . \quad (2)$$

These equations are derived from the dimensionless form, but an unknown factor having the dimension of length is omitted from the left-hand side and from the first group on the right-hand side of the equations. Because of this omission the equations are not dimensionless, and the proportionality constant α is expected to vary with the nature of the packing material and the units employed.

Degasification is a major mass-transfer process in industrial unit operation. Practical applications vary from degassing of petrochemicals and industrial fluids to deaeration of boiler feed water and potable liquids. Many application-oriented degassing studies can be found in the literature. Because of the unique OTEC conditions, only those studies involving vacuum deaeration and seawater applications are of relevance to this investigation; the studies include Knoedler and Bonilla⁷ (1954) on packed-column deaeration, Chambers⁸ (1959) on seawater spray deaeration, Eissenberg's review⁹ (1972) of the performance of deaerators in desalination pilot plants, and the vacuum degassing analysis by Rasguin et al.¹⁰ (1977).

Knoedler and Bonilla investigated vacuum degasification of water in a packed column. A closed test loop was constructed, and oxygen was used as the solute gas. Knoedler and Bonilla observed that end effects were appreciable and depended primarily on temperature. Below the loading point of liquid flow (i.e., liquid flow rate is less than $39 \times 10^3 \text{ kg/h}\cdot\text{m}^2$), their vacuum deaeration results for Stedman triangular packing were expressed by the following correlation:

$$\text{HTU} = 1.478 (L)^{0.3} . \quad (3)$$

A spray-type vacuum deaeration in connection with seawater desalination was investigated by Chambers.⁸ In his experiments, air was used as the solute gas with only the dissolved oxygen concentration measured by Winkler titration. Assumptions had to be made as to the rate of nitrogen release in determining the performance of the vacuum deaerator because oxygen and nitrogen are both sparsely soluble in water. The dissolved air content in the water at reduced pressures was computed from the dissolved oxygen measurements by using Henry's law of gas dissolution and Dalton's law of partial pressure for oxygen and nitrogen. Chambers⁸ found that this method was satisfactory for predicting the vacuum deaerator performance and reported that the HTU for the spray-type vacuum deaerator tested in his experiment varied from 21.3 to 45.7 cm (0.7 to 1.5 ft). His data showed that the value of HTU approached 45.7 cm (1.5 ft) as the pressure in the vacuum chamber was reduced. No correlation between HTU and vacuum pressure was presented.

Eissenberg⁹ (1972) has reviewed the operating experience of vacuum deaerators for seawater distillation plants; these data came from tests at plant facilities in San Diego, California; Freeport, Texas; Wrightsville Beach, North Carolina; and Oak Ridge, Tennessee. Because of the stringent degassing requirement for desalination plants, steam stripping was used. To achieve high rates of desorption, a combination of flashing feed, spray nozzles, and packed or tray columns was employed to increase the inter-phase area and mass-transfer coefficient. Eissenberg concluded that satisfactory deaerators for desalination plants could be designed using one or more mechanisms but that further experimental work was required to optimize costs and to design full-scale units.

Rasquim, Lynn, and Hanson¹⁰ (1977) studied various methods of dissolved air removal from water in packed columns through mathematical modeling. They studied cases of both countercurrent desorption (with and without steam stripping) and cocurrent gas desorption. They found that the gas removal rate in a two-stage cocurrent column was comparable to the countercurrent column with steam stripping and that less energy was consumed.

Very few studies have been performed on deaeration in a barometric intake system. Marchand¹¹ indicated that, from theoretical calculations,

only 3% deaeration was possible in the barometric intake configuration. However, he did not elaborate on the method of calculation or any kind of physical and geometrical effects on his calculation.

3. TEST LOOP DESIGN

The test loop design and description of the equipment for OTEC Gas Desorption Test Facility (OTEC-GDTF) was explained in detail in Vol. 1 of the ORNL study.¹ However, some modifications and expansion have taken place since then, particularly with the addition of a barometric intake configuration system to the gas desorption test column.

3.1 Modification of Dissolved Oxygen Measurement

As noted in the previous report,¹ the on-line dissolved-oxygen analyzer (Beckman Model 7002) was used for the direct-dissolved oxygen concentration measurement in water. However, the performance of the oxygen analyzer sensor in the vacuum environment of these experiments is subject to question. Because of this problem, water samples were collected under vacuum conditions in 1-L flasks, and they were then brought up to atmospheric conditions (see oxygen-measuring station in the following subsection). Samples then were transferred into 300-cc biological oxygen demand (BOD) bottles, and an oxygen analyzer (Yellow Springs Instrument Model 57) measured the dissolved-oxygen content of water in parts per million. As a supplemental check for verification and calibration of the sampling technique, water samples in BOD bottles were periodically sent to a chemical laboratory for dissolved-oxygen content analysis by the Winkler wet titration method.

3.2 Description of Equipment

The OTEC-GDTF used in this investigation is shown in a flow diagram (Fig. 1) and in an overall view (Fig. 2). These major loop components are explained in detail in Sects. 3.3 through 3.10: (1) test section, (2) vacuum system, (3) lower barometric-leg water storage tank, (4) upper water storage tank and pumps, (5) oxygen-sampling stations, and (6) barometric-leg materials.

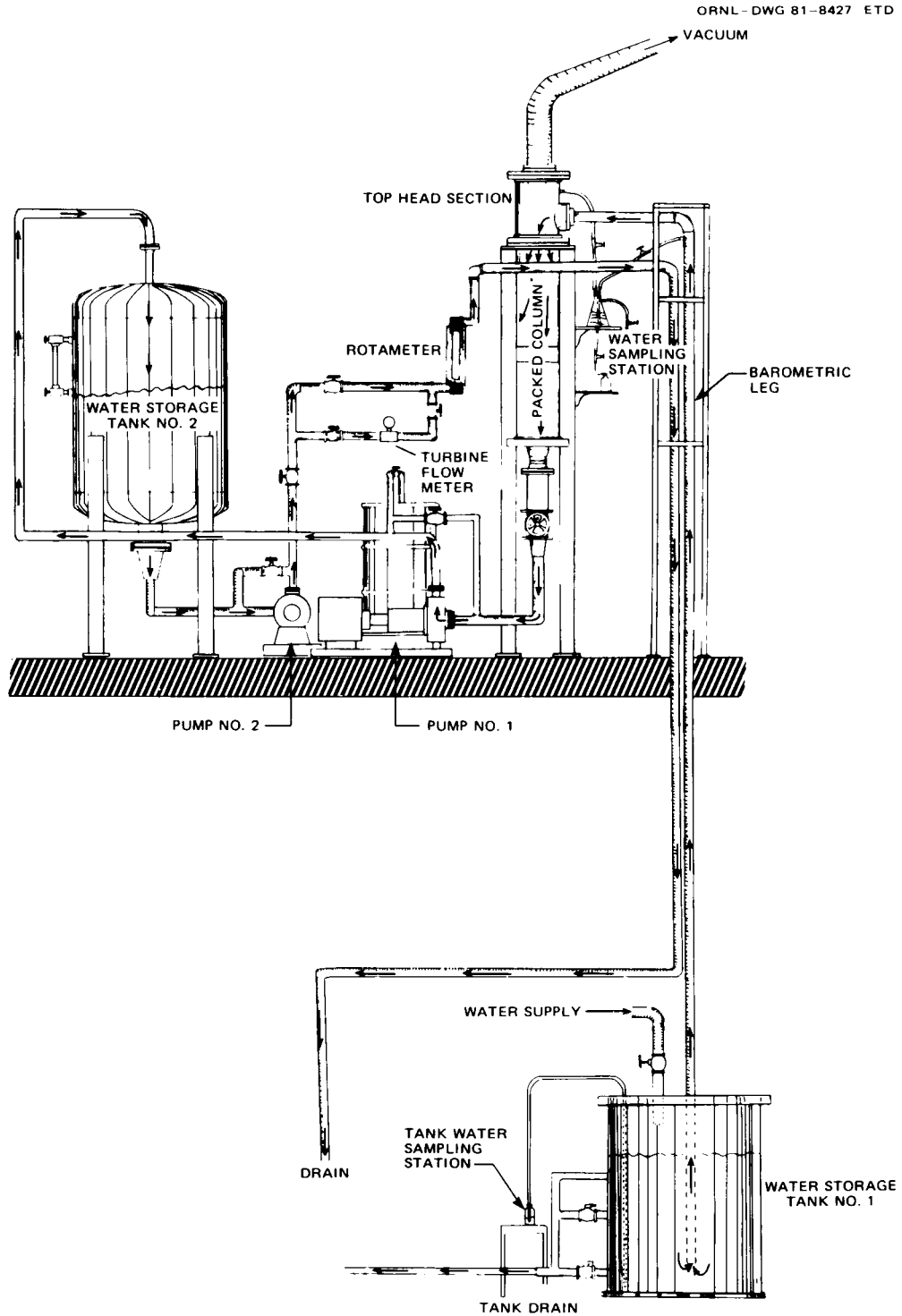


Fig. 1. Generalized flow diagram of OTEC packed column-barometric intake facility.

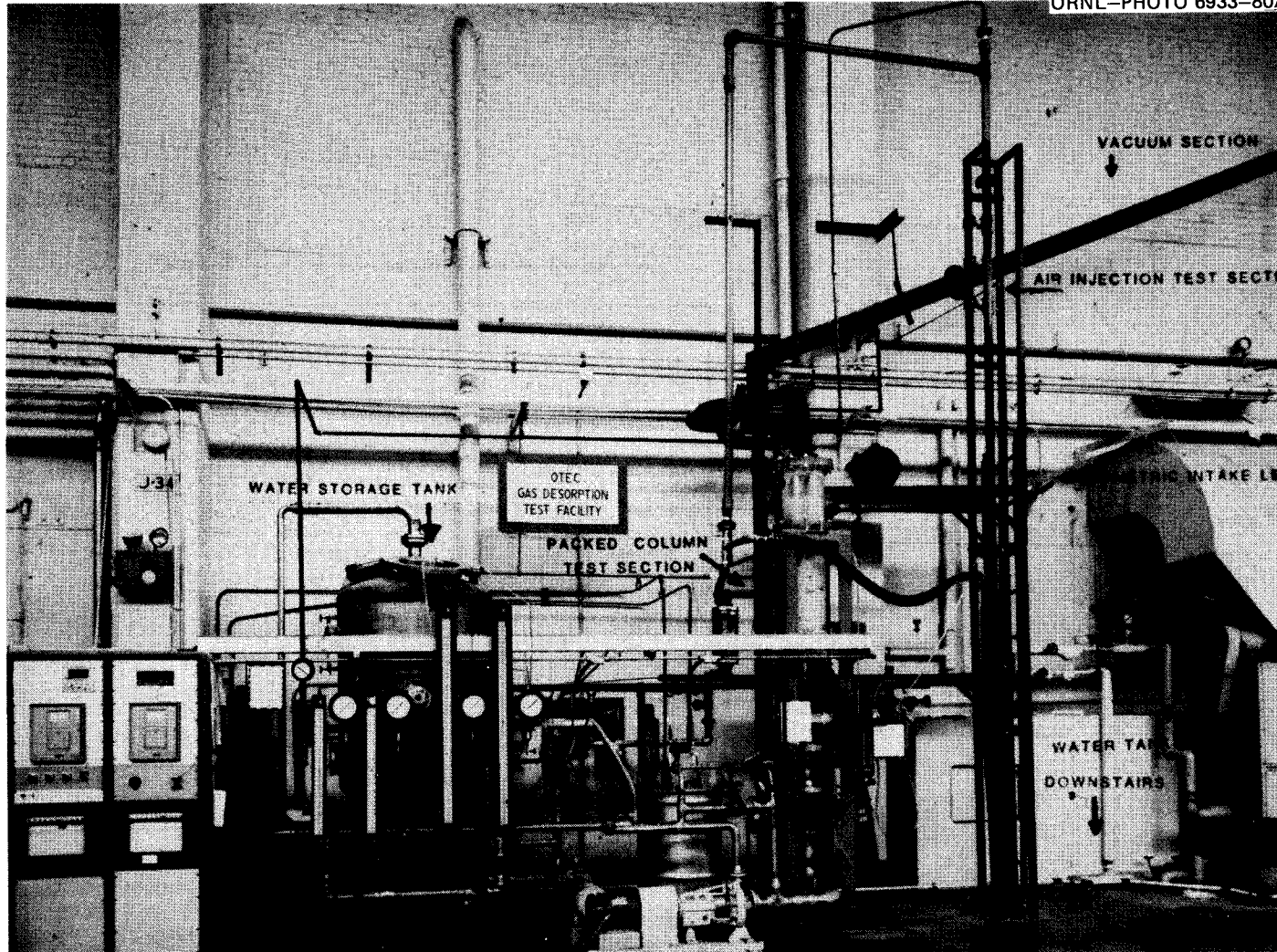


Fig. 2. OTEC Gas Desorption Test Facility.

3.3 General Flow Description

Flow directions for the barometric intake system are indicated by arrows in the simplified schematic diagram (Fig. 3). The experimental system consists of four components: a water holding tank equipped with manual level control to maintain different water heights, a barometric leg, a sampling station, and a water-returning system. Two separated systems are used for aeration when the system is in closed-loop operation

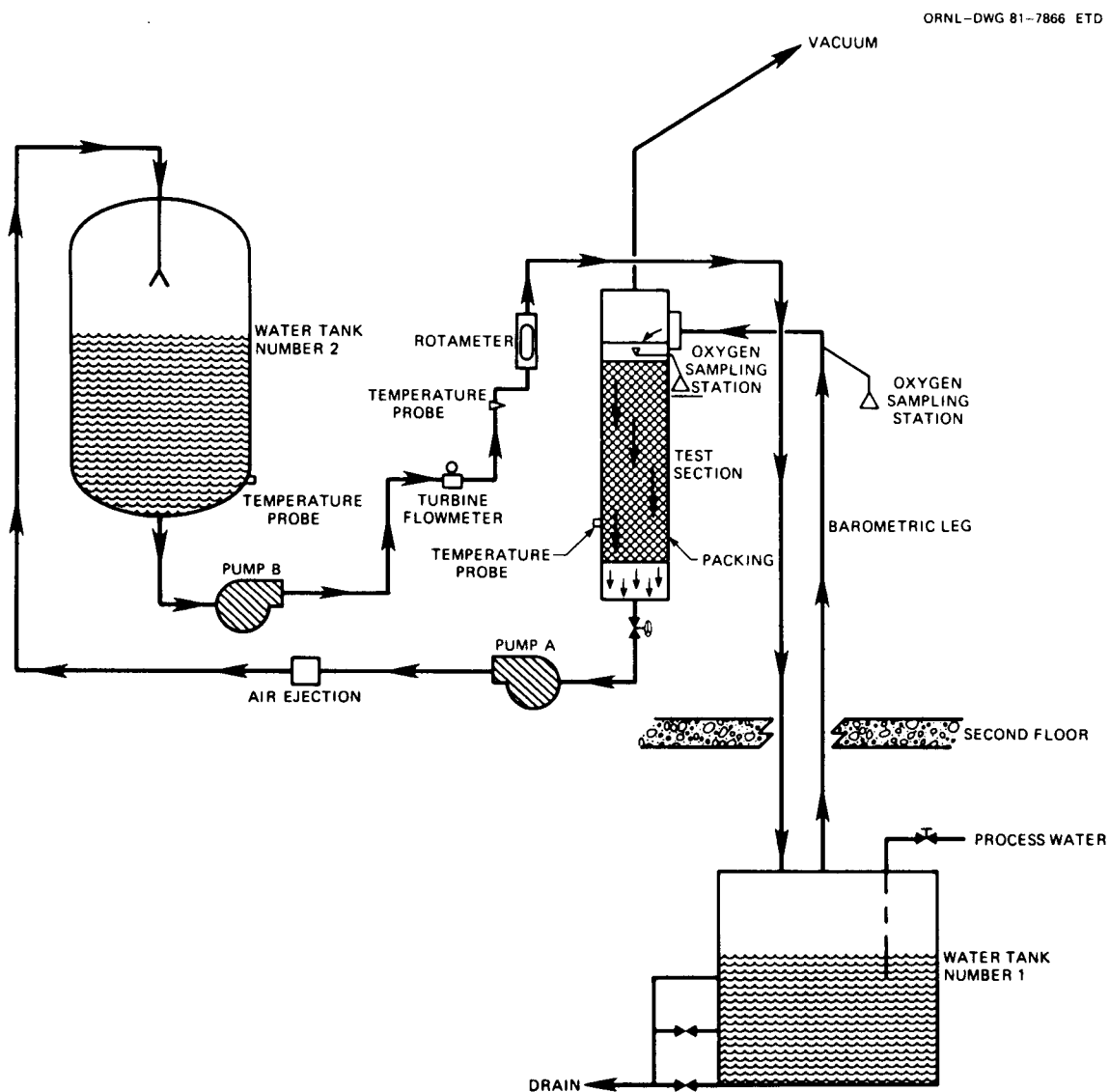


Fig. 3. Barometric intake simplified flow diagram.

mode, and a building water line with a hand-regulated valve directly provides source water in once-through operations. The loop is designed to operate under vacuum conditions and up to 310 kPa.

In the closed loop, water storage tank No. 1 (Fig. 3) was filled to the desired height with air-saturated building water. Through the use of a vacuum system, water was pulled up into the barometric leg. Water samples were taken as it entered the barometric leg and again at the end of barometric intake leg as the water left to go into the test column. From the test column, water was recirculated into the holding tank for closed-loop operation or into a building drain for open-loop operation. During the closed-loop operation, air was continuously injected into the system by an array of air stones (Kordon Corporation No. 62501). In the open-loop operation mode, air-saturated water was continuously fed from the building water supply at a rate equal to that being drained. A manually operated valve located at the top of holding tank No. 1 was used to maintain constant liquid level in the tank. Excess water entering the tank was drained through valves located on the side of the tank (Fig. 4). Water flow was measured by a turbine flowmeter (FLOW TECHNOLOGY) as it entered tank No. 2, and its temperature was measured by thermistors (Yellow Springs Instrument Company).

3.4 Test Section Packed Column

The primary function of the test section column in the barometric-leg experiment is to provide a measuring station for temperature and a visual liquid flow level. As the water leaves the barometric leg, it enters the top-head section of the test section and passes through the main body of the column where the temperature of the liquid is measured. The top-head section also provides the connection to the vacuum source. The height of water in the column also provides head pressure for pump A. The column is made of clear plastic, and O-ring gaskets are used on all removable connections.

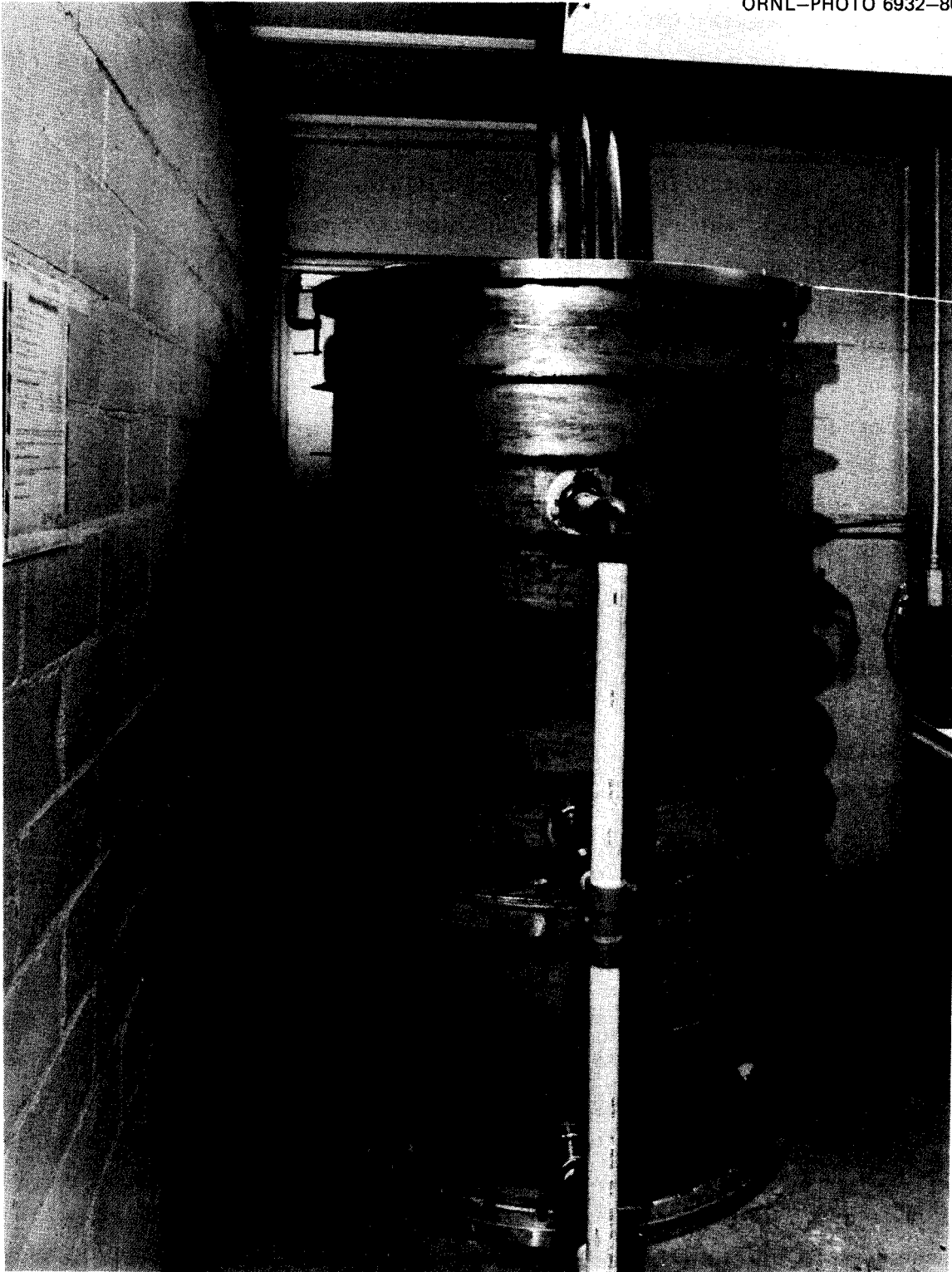


Fig. 4. Water storage tank.

3.5 Flow Control Water Pumps

The water from the column was circulated by a 3.73-kW (5-hp) centrifugal pump (Allis Chamber 042-1-99-51) into tank No. 2, which is used for secondary aeration for the closed loop. Water from tank No. 2 was pumped by pump B, a 1.12-kW (1.5-hp) centrifugal pump, through a turbine flow meter (1-in. Flow Technology Model No. FT-16) and rotameter (Fischer Serial No. XII-4425/2) back into the lower barometric-leg holding tank No. 1 for closed-loop operation. Water was discharged to the building drain system directly instead of to holding tank No. 1 in the case of open-loop operation.

3.6 Oxygen-Measuring Station

The oxygen-measuring station consists of a 1-L flask connected to the top of the barometric leg by 0.95-cm-ID Tygon hose (Fig. 1). The flask is also connected and valved to the vacuum system, atmosphere, and a BOD bottle drain point. These connections give the station flexibility. The vacuum line equalizes the pressure of the flask to that of the barometric leg while under vacuum. The atmospheric connection enables the water sample in the flask to be brought to atmospheric pressure without adding any oxygen to the sample, and finally the valved drain enables the flask's content to empty into a BOD bottle. This sampling procedure is similar to the one employed by Knoedler and Bonilla⁷ in their study of vacuum deaeration. The bottles can be analyzed by either the Winkler wet titration method or an oxygen analyzer (Yellow Springs Model 57 Oxygen Analyzer). All valves are 3/8-in. tubing-connected vacuum bellow valves (Hoke Model No. 4213Q64). All tubing is Tygon 3/8-in. ID and 5/8-in. OD.

3.7 Vacuum System

In the gas removal system, a 10.2-cm-diam (4-in.) steel line followed by a 15.24-cm-diam (6-in.) pipe connects the top of the desorption column to the vacuum equipment. An existing two-stage steam-jet ejector in the building serves as the vacuum source. The ejector has a name plate capacity of removing 13.6 kg/h (30 lb/h) of water vapor and 1.36 kg/h (3 lb/h)

of air at 1.35 kPa abs (0.4 in. Hg abs). The vacuum pressure is controlled by a vacuum pressure regulator. It is necessary to bleed a small amount of air into the vacuum piping system to obtain satisfactory control of the vacuum pressure under varying test conditions.

3.8 Barometric-Leg Water Holding Tank

The barometric-leg water storage tank (Fig. 4) was fabricated from 1.27-cm stainless steel plate rolled into a drum 1.04 m in diameter and 1.83 m in height. This tank serves as a storage reservoir for the water at full air saturation just before it enters the vertical barometric leg. The tank is equipped with three drain ports at 11.4, 76.20, and 137.2 cm from the bottom. Two of these three are valved lines, and the third is simply an overflow protection drain. These two drain lines enable the tank to maintain a constant level, while the outside building water enters the tank from a 3.81-cm process water line located at the top of the tank and regulated by a globe valve. The tank is also a place of water aeration and contains an array of air stones (Kordon Corporation) that are connected to the building air supply at 800 kPa.

3.9 Barometric Intake System

A standard start-up procedure was implemented for each day of experimental tests. All drains on storage tank No. 1 were closed, and the building water fill line was opened. After a closely estimated water level was achieved, the vacuum valve was opened and set on its desired pressure for that day's run. As the barometric leg began to discharge water into the test column, pump A was turned on and the water level in the column was set to zero. In open-loop operations, all water was to be drained after one pass through the loop; the building water fill line again was turned on and regulated to maintain a constant level in water storage tank No. 1.

3.10 Steady-State Operation

After start-up, a constant level was maintained in both water tank No. 1 in the packed column. Temperature and vacuum pressures were monitored to determine when steady-state conditions existed.

Steady state was assumed when there was no significant change in temperature ($\pm 0.1^\circ\text{C}$) and flow rate changes were less than $\pm 2\%$ throughout the system over a 10-min span. Once steady state was achieved, the following data were recorded: (1) flow rate through the barometric leg, (2) temperature of the water in the barometric leg, (3) parts per million of oxygen content of the water in storage tank No. 1, (4) water samples taken as it reached the top of the barometric leg (7.8 to 8.8 m from the water level in tank No. 2), and (5) the system vacuum pressure. These experimental data were fed to a computer to calculate the deaeration effectiveness of barometric intake configuration.

After all data were recorded and water samples were taken for analysis, the water flow rate through the barometric leg was changed; adjustments were made until a new steady state condition was achieved. Experimental data were again recorded, and the procedure was repeated.

4. RESULTS AND DISCUSSION

4.1 Results of Vacuum Deaeration in a Packed Column

Vacuum deaeration of water was studied in a 28-cm-ID tower filled with two kinds of packings: ceramic Raschig ring and plastic pall rings. Packing heights were varied from 0 to 90 cm, liquid rates from 34,000 to 146,000 kg/h·m², and the column vacuum pressure from 3.4 to 34 kPa abs. Liquid samples, taken at the top of the packing and at the outlet of the tower, were analyzed by an oxygen analyzer to determine the concentration of dissolved oxygen.

The first series of runs (110 in all) was completed, and the results were presented in Vol. 1 of this report.¹ In this first series of runs, the packing was 3.81-cm ceramic Raschig rings, and the measured deaeration used for calculation of coefficients included deaeration that takes place on the packing as well as between the sensor of the oxygen analyzer and the top of the packed column. Because of the end effect, that is, the additional deaeration that occurs in the inlet distributor and the deaerated water reservoir of the packed column, data obtained in the first series should apply only to the particular conditions of the test setup.

A new group of runs (121 in all) was then made in which the liquid entering the packing was sampled at the top of the packing by using the collecting flask and BOD bottle as described previously. These runs were made with 2.54-cm plastic pall rings (Test Series 2) and 3.81-cm plastic pall rings (Test Series 3). Although the method of correlation presented is based on the first series runs, the quantitative basis for the prediction of mass-transfer coefficients is the new group of 121 runs. Data obtained in the latter group are presented in Tables 1 through 4. Data on the liquid film coefficient of the desorption of air from water for 2.54- and 3.81-cm plastic pall rings are shown in Figs. 5 and 6. Most of the test data were obtained at temperatures within a few degrees of 25°C, and the values reported have been corrected to 25°C by the use of empirical relation.⁶

The effect of vacuum pressure is indicated by the data of Fig. 7, taken from Test Series 3 with 3.81-cm plastic pall rings.

Table 1. Test Series 2 (1-in. pall rings)^a

TEST	L	TEMP	PAIR	XI	XØ	XE	NTU	Σ	D	SC	PACKING HEIGHT
701	.176E+05	82.1	5.86	4.46	4.43	1.57	.01	0.67	.934E-04	.351E+03	0.0
702	.176E+05	82.1	5.86	4.68	3.46	1.57	.50	26.07	.934E-04	.350E+03	11.0
703	.172E+05	82.1	5.81	4.35	2.72	1.56	.88	37.47	.933E-04	.351E+03	22.0
704	.175E+05	82.0	5.81	4.63	2.36	1.56	1.34	49.03	.932E-04	.351E+03	33.0
705	.210E+05	81.9	5.83	4.83	4.39	1.57	.14	9.11	.932E-04	.352E+03	0.0
706	.210E+05	82.0	5.83	4.96	3.21	1.57	.72	35.28	.932E-04	.352E+03	22.0
707	.210E+05	82.0	5.83	5.08	3.46	1.57	.62	31.89	.932E-04	.352E+03	11.0
708	.210E+05	82.1	5.89	4.82	2.46	1.58	1.30	48.96	.934E-04	.351E+03	33.0
709	.242E+05	81.7	5.88	5.51	4.60	1.58	.26	16.52	.929E-04	.354E+03	0.0
710	.242E+05	81.6	5.97	5.63	3.74	1.61	.63	33.57	.927E-04	.355E+03	11.0
711	.242E+05	81.6	5.97	5.40	3.11	1.61	.93	42.41	.927E-04	.355E+03	22.0
712	.242E+05	81.7	5.88	5.59	2.75	1.58	1.23	50.81	.929E-04	.354E+03	33.0
713	.273E+05	81.7	5.86	5.59	4.78	1.58	.23	14.49	.929E-04	.354E+03	0.0
714	.273E+05	81.8	5.86	5.52	3.68	1.58	.63	33.33	.930E-04	.353E+03	11.0
715	.273E+05	81.7	5.86	5.31	3.07	1.58	.92	42.18	.929E-04	.354E+03	22.0
716	.273E+05	81.8	5.86	5.51	2.80	1.58	1.17	49.18	.929E-04	.354E+03	33.0
721	.179E+05	83.6	3.97	4.03	3.80	1.05	.08	5.71	.953E-04	.338E+03	0.0
722	.179E+05	83.6	3.97	3.95	2.97	1.05	.41	24.81	.953E-04	.338E+03	11.0
723	.179E+05	83.6	3.91	4.01	2.25	1.03	.90	43.89	.952E-04	.338E+03	22.0
724	.179E+05	83.6	3.91	4.00	1.90	1.03	1.23	52.50	.952E-04	.338E+03	33.0
725	.210E+05	83.5	3.90	5.05	4.08	1.03	.28	19.21	.952E-04	.338E+03	0.0
726	.210E+05	83.5	3.90	5.05	3.05	1.03	.69	39.60	.952E-04	.338E+03	11.0
727	.210E+05	83.4	3.92	5.12	2.30	1.04	1.17	55.08	.950E-04	.339E+03	22.0
728	.210E+05	83.4	3.90	4.99	1.95	1.03	1.46	60.92	.951E-04	.339E+03	33.0
729	.242E+05	83.8	3.90	5.08	3.95	1.03	.33	22.24	.955E-04	.336E+03	0.0
730	.242E+05	83.8	3.90	5.03	3.00	1.03	.71	40.36	.955E-04	.336E+03	11.0
731	.242E+05	83.8	3.90	5.05	2.40	1.03	1.08	52.48	.955E-04	.336E+03	22.0
732	.242E+05	83.8	3.92	4.95	2.00	1.03	1.40	59.60	.955E-04	.336E+03	33.0
742	.179E+05	82.0	7.70	5.60	5.16	2.07	.13	7.86	.932E-04	.351E+03	0.0
743	.179E+05	82.0	7.70	5.30	3.67	2.07	.70	30.75	.932E-04	.351E+03	14.0
744	.179E+05	81.9	7.71	5.56	2.90	2.07	1.44	47.84	.932E-04	.352E+03	33.0
745	.210E+05	82.1	7.67	5.98	5.90	2.06	.02	1.34	.933E-04	.351E+03	0.0
746	.210E+05	82.1	7.70	5.72	3.76	2.06	.77	34.27	.934E-04	.351E+03	14.0
747	.210E+05	81.9	7.71	5.65	2.99	2.07	1.36	47.08	.931E-04	.352E+03	33.0
748	.242E+05	81.6	7.72	5.99	5.02	2.08	.29	16.19	.927E-04	.355E+03	0.0
749	.242E+05	81.7	7.71	5.55	3.75	2.08	.73	32.43	.929E-04	.354E+03	14.0
750	.242E+05	81.7	7.71	5.85	3.12	2.08	1.29	46.67	.929E-04	.354E+03	33.0
751	.271E+05	81.6	7.83	5.68	4.97	2.11	.22	12.50	.927E-04	.355E+03	0.0
752	.273E+05	81.4	7.86	5.64	3.88	2.12	.69	31.21	.926E-04	.356E+03	14.0
753	.273E+05	81.4	7.86	5.95	3.20	2.12	1.27	46.22	.926E-04	.356E+03	33.0

Table 1 (continued)

TEST	L	TEMP	PAIR	XI	XØ	XE	NTU	%	D	SC	PACKING HEIGHT
757	.200E+05	82.4	2.03	4.27	3.87	0.54	.11	9.37	.937E-04	.348E+03	0.0
758	.200E+05	82.2	1.92	4.20	2.37	0.52	.69	43.57	.935E-04	.350E+03	14.0
759	.200E+05	82.3	1.92	3.96	1.50	0.51	1.25	62.12	.936E-04	.349E+03	33.0
760	.231E+05	82.2	1.88	4.66	3.80	0.50	.23	18.45	.935E-04	.350E+03	0.0
761	.231E+05	82.2	1.95	4.53	2.40	0.52	.76	47.02	.935E-04	.350E+03	14.0
762	.231E+05	82.2	1.95	4.61	1.60	0.52	1.33	65.29	.935E-04	.350E+03	33.0
763	.261E+05	82.1	1.90	4.85	3.68	0.51	.31	24.12	.934E-04	.350E+03	0.0
764	.263E+05	82.1	1.88	4.56	2.40	0.50	.76	47.37	.934E-04	.350E+03	14.0
765	.261E+05	82.2	1.89	4.57	1.50	0.51	1.41	67.18	.935E-04	.350E+03	33.0
766	.210E+05	83.1	2.07	4.43	3.70	0.55	.21	16.48	.947E-04	.341E+03	0.0
767	.210E+05	82.6	2.29	4.44	2.36	0.61	.78	46.85	.940E-04	.346E+03	14.5
768	.210E+05	82.6	2.29	4.45	1.42	0.61	1.56	68.09	.940E-04	.346E+03	33.0
769	.242E+05	82.6	2.19	4.68	3.85	0.58	.23	17.74	.940E-04	.346E+03	0.0
770	.242E+05	82.7	2.19	4.53	2.32	0.58	.82	48.79	.941E-04	.345E+03	14.5
771	.242E+05	82.7	2.29	4.46	1.50	0.61	1.46	66.37	.941E-04	.345E+03	33.0
772	.273E+05	81.6	2.22	4.83	3.80	0.60	.28	21.33	.928E-04	.355E+03	0.0
773	.273E+05	81.6	2.08	4.72	2.39	0.56	.82	49.36	.927E-04	.355E+03	14.5
774	.273E+05	81.6	2.05	4.73	1.52	0.55	1.46	67.86	.928E-04	.355E+03	33.0
775	.368E+05	81.8	2.16	4.77	3.78	0.58	.27	20.75	.929E-04	.354E+03	0.0
776	.365E+05	81.7	2.04	4.76	2.50	0.55	.77	47.48	.929E-04	.354E+03	14.5
777	.365E+05	81.6	2.02	4.67	1.64	0.54	1.33	64.88	.927E-04	.355E+03	33.0

^aVariables are expressed in the following units:

$$L = \text{lb/h}\cdot\text{ft}^2$$

$$\text{Temp} = \text{°F}$$

$$P_{\text{air}} = \text{in. Hg}$$

$$D = \text{ft}^2/\text{h}$$

$$\text{Packing height} = \text{in.}$$

Table 2. Test Series 2^a

TEST SERIES	L	PAIR	TEMP	HTU	HTU25	MU	KLA	L/MU	K/DSC	END EFF
701 - 704	.175E+05	5.84	82.1	2.093	2.23	2.04	.134E+03	.857E+04	.643E+05	0.640
705 - 708	.210E+05	5.85	82.0	2.560	2.72	2.04	.132E+03	.103E+05	.634E+05	4.932
709 - 712	.242E+05	5.92	81.7	2.865	3.03	2.05	.136E+03	.118E+05	.651E+05	9.773
713 - 716	.273E+05	5.86	81.8	2.942	3.12	2.04	.149E+03	.134E+05	.716E+05	9.433
721 - 724	.179E+05	3.94	83.6	2.329	2.52	2.00	.123E+03	.892E+04	.591E+05	1.798
725 - 728	.210E+05	3.90	83.5	2.268	2.46	2.00	.149E+03	.105E+05	.714E+05	7.998
729 - 732	.242E+05	3.91	83.8	2.556	2.78	2.00	.152E+03	.121E+05	.729E+05	10.431
742 - 744	.179E+05	7.70	82.0	2.115	2.25	2.04	.136E+03	.876E+04	.651E+05	3.532
745 - 747	.210E+05	7.69	82.0	2.083	2.21	2.04	.162E+03	.103E+05	.777E+05	2.227
748 - 750	.242E+05	7.72	81.7	2.756	2.92	2.05	.141E+03	.118E+05	.677E+05	9.687
751 - 753	.272E+05	7.85	81.5	2.639	2.79	2.05	.166E+03	.133E+05	.798E+05	7.363
757 - 759	.200E+05	1.96	82.3	2.436	2.60	2.03	.132E+03	.982E+04	.632E+05	4.322
760 - 762	.231E+05	1.93	82.2	2.510	2.67	2.03	.148E+03	.114E+05	.711E+05	7.659
763 - 765	.261E+05	1.89	82.2	2.507	2.67	2.03	.167E+03	.128E+05	.802E+05	9.234
766 - 768	.210E+05	2.22	82.8	2.036	2.19	2.02	.166E+03	.104E+05	.794E+05	4.935
769 - 771	.242E+05	2.22	82.7	2.228	2.39	2.02	.174E+03	.120E+05	.837E+05	6.558
772 - 774	.273E+05	2.11	81.6	2.329	2.46	2.05	.189E+03	.133E+05	.905E+05	8.025
775 - 777	.366E+05	2.07	81.7	2.610	2.76	2.05	.225E+03	.178E+05	.108E+06	8.863

^aVariables are expressed in the following units:

$$L = \text{lb/h}\cdot\text{ft}^2$$

$$P_{\text{air}} = \text{in. Hg}$$

$$\text{Temp} = ^\circ\text{F}$$

$$\text{HTU} = \text{ft}$$

$$\text{HTU}_{25} = \text{ft}$$

$$\mu = \text{lbm/ft}\cdot\text{h}$$

$$k_{\text{La}} = \text{lb mole}/(\text{h}\cdot\text{ft}^3) \quad (\text{lb mole}/\text{ft}^3)$$

$$L/\mu = 1/\text{ft}$$

$$k/\text{DSc} = 1/\text{ft}^2$$

$$\text{End Eff} = \text{in.}$$

Table 3. OTEC gas desorption test loop Test Series 3 (1.5-in. pall rings)^a

TEST	L	TEMP	PAIR	XI	X0	XE	NTU	Σ	D	SC	PACKING HEIGHT
900	.179E+05	71.4	1.09	3.96	3.96	0.32	.00	0.00	.798E-04	.469E+03	0.0
901	.179E+05	71.4	1.09	4.09	3.10	0.32	.30	24.21	.798E-04	.469E+03	11.0
902	.179E+05	71.4	1.09	4.00	2.26	0.32	.64	43.50	.798E-04	.469E+03	22.0
903	.179E+05	71.5	1.09	3.79	1.60	0.32	1.00	57.78	.799E-04	.469E+03	33.0
904	.368E+05	70.1	1.06	4.88	4.41	0.32	.11	9.63	.784E-04	.486E+03	0.0
905	.368E+05	70.1	1.06	4.87	3.51	0.32	.35	27.93	.784E-04	.486E+03	11.0
906	.368E+05	70.2	1.22	5.10	2.75	0.36	.69	46.08	.784E-04	.485E+03	22.0
907	.368E+05	70.2	1.12	4.82	2.18	0.33	.89	54.77	.784E-04	.485E+03	33.0
908	.395E+05	71.4	1.09	4.64	4.11	0.32	.13	11.42	.798E-04	.470E+03	0.0
909	.395E+05	71.4	1.09	3.36	2.37	0.32	.39	29.46	.798E-04	.469E+03	11.0
910	.395E+05	71.4	1.09	4.75	2.50	0.32	.71	47.37	.798E-04	.469E+03	22.0
911	.395E+05	71.4	1.09	4.76	2.11	0.32	.91	55.67	.798E-04	.469E+03	33.0
912	.210E+05	72.1	4.32	6.02	4.39	1.27	.42	27.08	.805E-04	.462E+03	11.0
913	.210E+05	72.1	4.40	6.06	2.95	1.29	1.06	51.32	.806E-04	.461E+03	33.0
914	.210E+05	73.4	4.46	5.95	4.35	1.29	.42	26.89	.822E-04	.445E+03	11.5
915	.210E+05	73.4	4.58	5.91	2.96	1.33	1.03	49.92	.821E-04	.446E+03	33.0
916	.242E+05	72.0	4.39	6.12	4.46	1.29	.42	27.12	.805E-04	.462E+03	11.0
917	.242E+05	72.0	4.40	6.12	3.48	1.29	.79	43.14	.805E-04	.462E+03	22.0
918	.242E+05	72.0	4.44	6.29	3.07	1.31	1.04	51.19	.805E-04	.462E+03	33.0
919	.315E+05	73.3	4.36	6.39	4.55	1.27	.44	28.79	.820E-04	.446E+03	11.0
920	.315E+05	73.4	4.36	6.29	3.52	1.26	.80	44.04	.821E-04	.446E+03	22.0
921	.315E+05	73.4	4.40	6.01	3.11	1.28	.95	48.25	.821E-04	.446E+03	33.0
922	.315E+05	71.2	4.39	6.47	4.56	1.30	.46	29.52	.796E-04	.472E+03	11.0
923	.315E+05	71.2	4.39	6.39	3.52	1.30	.83	44.91	.796E-04	.472E+03	22.0
924	.315E+05	71.2	4.49	6.40	3.11	1.33	1.05	51.41	.796E-04	.472E+03	33.5
925	.315E+05	73.9	4.36	6.10	4.32	1.26	.46	29.18	.827E-04	.439E+03	11.0
926	.315E+05	73.8	4.56	6.09	3.39	1.32	.83	44.33	.826E-04	.440E+03	22.0
927	.315E+05	73.9	4.56	6.04	2.96	1.32	1.06	50.99	.827E-04	.439E+03	33.0
928	.242E+05	72.5	8.25	6.39	5.12	2.41	.38	19.87	.811E-04	.456E+03	12.3
929	.242E+05	72.5	8.31	6.70	4.08	2.43	.95	39.10	.811E-04	.456E+03	33.0
930	.242E+05	72.4	8.28	6.41	5.15	2.42	.38	19.66	.809E-04	.457E+03	10.5
931	.242E+05	72.4	8.28	6.55	4.43	2.42	.72	32.37	.809E-04	.457E+03	22.0
932	.273E+05	73.4	8.26	6.31	5.12	2.40	.36	18.86	.821E-04	.446E+03	11.5
933	.273E+05	73.4	8.38	6.40	4.00	2.43	.93	37.50	.821E-04	.446E+03	33.0
934	.273E+05	72.4	8.28	6.98	5.33	2.42	.45	23.64	.810E-04	.457E+03	11.0
935	.273E+05	72.4	8.28	6.69	3.89	2.42	1.07	41.85	.810E-04	.457E+03	33.0
936	.315E+05	73.6	8.38	6.72	5.15	2.43	.46	23.36	.824E-04	.443E+03	11.0
937	.315E+05	73.6	8.40	6.70	4.35	2.43	.80	35.07	.824E-04	.443E+03	23.0
938	.315E+05	72.4	8.28	6.91	5.11	2.42	.51	26.05	.809E-04	.457E+03	11.0
939	.315E+05	72.5	8.26	7.00	3.93	2.42	1.11	43.86	.811E-04	.456E+03	34.0

Table 3 (continued)

TEST	L	TEMP	PAIR	XI	XØ	XE	NTU	Z	D	SC	PACKING HEIGHT
940	.368E+05	73.6	8.40	6.91	5.20	2.43	.48	24.75	.824E-04	.443E+03	11.0
941	.368E+05	73.6	8.40	6.65	4.36	2.43	.78	34.44	.823E-04	.443E+03	22.0
942	.368E+05	73.6	8.40	6.68	3.96	2.43	1.02	40.72	.823E-04	.443E+03	33.0
943	.158E+05	67.4	8.38	6.81	5.40	2.57	.40	20.70	.749E-04	.529E+03	11.0
944	.158E+05	67.4	8.38	6.86	4.40	2.57	.85	35.86	.749E-04	.529E+03	22.0
945	.158E+05	67.4	8.38	6.90	4.05	2.57	1.07	41.30	.749E-04	.529E+03	33.5

^aVariables are expressed in the following units:

$$L = \text{lb/h}\cdot\text{ft}^2$$

$$\text{Temp} = ^\circ\text{F}$$

$$P_{\text{air}} = \text{in. Hg}$$

$$D = \text{ft}^2/\text{h}$$

$$\text{Packing height} = \text{in.}$$

The values of HTU scatter between 70 to 100 cm at the testing vacuum pressure range. The same conclusion was obtained from the data of the first series with 3.81-cm ceramic Raschig rings.¹ The practical conclusion is that HTU is independent of vacuum pressure. The data on HTU of deaeration in 2.54- and 3.81-cm plastic pall rings are shown in Figs. 8 and 9, respectively. These figures are plotted on log-log scale, and the points scatter around a straight line up to quite high values of the liquid flow rate.

Because of channeling of liquid near the walls of the packed column, it is desirable to use an experimental column with a ratio of diameter to packing dimension of at least 8:1 if the results are to be considered representative of large scale operation (especially if the packed depth is sufficiently great to permit channeling to develop). With the 12-in. (30-cm) tower of this investigation, the minimum ratio was exceeded for all packings used.

The packed height was likewise a compromise and was usually less than common in industrial practice. A large packed height results in more desorption and greater accuracy in measuring the rate of deaeration, but the driving force at the bottom of the column is then very small and difficult

Table 4. Test Series 3^a

TEST SERIES	L	PAIR	TEMP	HTU	HTU25	MU	KLA	L/MU	K/DSC	END EFF
900 - 903	.179E+05	1.09	71.5	2.754	2.57	2.33	.104E+03	.765E+04	.501E+05	-0.450
904 - 907	.368E+05	1.12	70.2	3.435	3.15	2.37	.172E+03	.155E+05	.827E+05	4.492
908 - 911	.395E+05	1.09	71.4	3.461	3.22	2.33	.183E+03	.169E+05	.881E+05	5.752
912 - 915	.210E+05	4.44	72.7	2.907	2.75	2.30	.116E+03	.922E+04	.563E+05	3.424
916 - 918	.242E+05	4.41	72.0	2.971	2.79	2.32	.131E+03	.104E+05	.628E+05	4.750
919 - 927	.315E+05	4.43	72.8	3.287	3.12	2.29	.154E+03	.139E+05	.752E+05	8.098
928 - 931	.242E+05	8.28	72.4	3.127	2.95	2.30	.124E+03	.105E+05	.596E+05	3.410
932 - 935	.273E+05	8.30	72.9	3.070	2.91	2.29	.143E+03	.118E+05	.682E+05	3.730
936 - 939	.315E+05	8.33	73.0	3.083	2.93	2.29	.164E+03	.137E+05	.783E+05	6.839
940 - 942	.368E+05	8.40	73.6	3.383	3.24	2.27	.175E+03	.162E+05	.839E+05	8.953
943 - 945	.158E+05	8.38	67.4	2.808	2.49	2.47	.901E+02	.639E+04	.433E+05	4.019

^aVariables are expressed in the following units:

$$L = \text{lb/h}\cdot\text{ft}^2$$

$$P_{\text{air}} = \text{in. Hg}$$

$$\text{Temp} = ^\circ\text{F}$$

$$\text{HTU} = \text{ft}$$

$$\text{HTU25} = \text{ft}$$

$$\mu = \text{lbm/h}\cdot\text{ft}$$

$$k_{\text{La}} = \text{lb mole}/(\text{h}\cdot\text{ft}^3)(\text{lb mole}/\text{ft}^3)$$

$$L/\mu = 1/\text{ft}$$

$$k/\text{DSc} = 1/\text{ft}^2$$

$$\text{End Eff} = \text{in.}$$

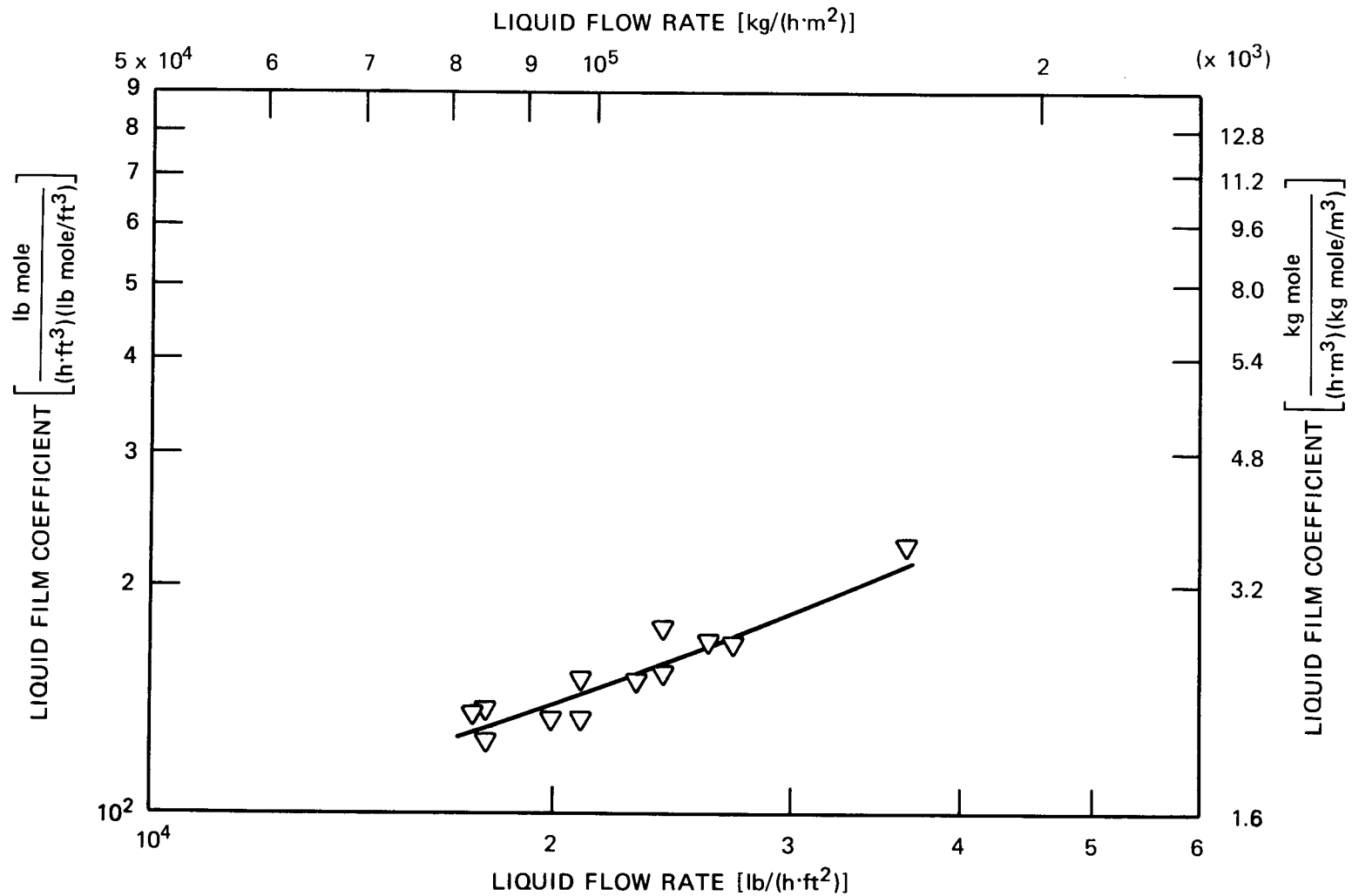


Fig. 5. Liquid film coefficient vs liquid flow rate when 2.54-cm (1-in.) plastic pall ring is used.

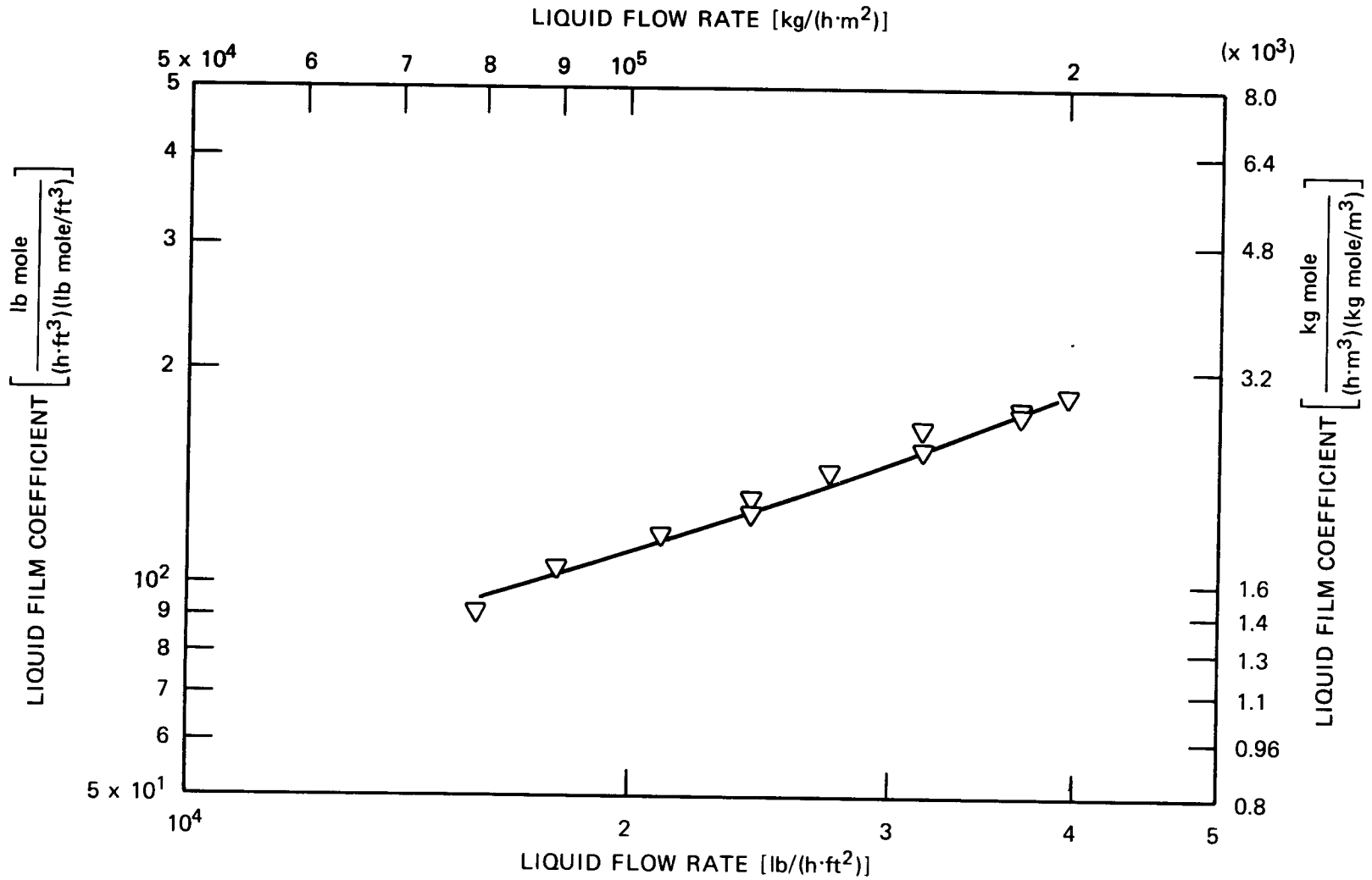


Fig. 6. Liquid film coefficient vs liquid flow rate when 3.81-cm (1.5-in.) plastic pall ring is used.

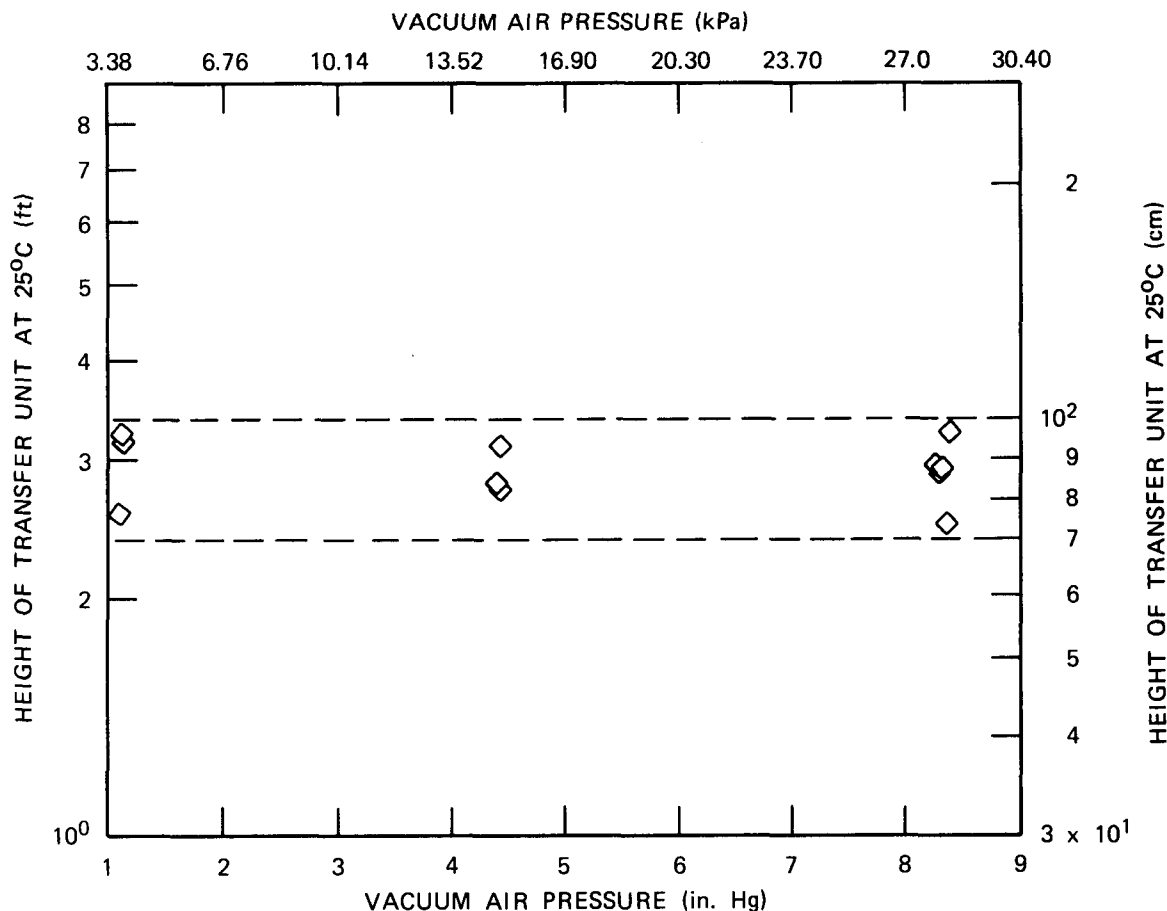


Fig. 7. Effect of vacuum pressure on HTU at constant temperature.

to measure with accuracy. A very short packed height results in large driving forces at both ends of the column, but the amount of air transferred is small and an appreciable fraction of the total transfer may take place at the top and bottom of the packing in the regions of spray and splashing. In our investigation, the packing height was varied from 15 to 90 cm.

The effect of packed height on NTU was investigated in our studies by taking liquid samples just above and below the packing. That end effects have indeed been minimized is evident from Fig. 10 (Tests 701 through 704 and 900 through 903); it shows a negligible variation of NTU at zero intercept with packing heights, indicating uniform liquid distribution and liquid-gas-interfacial area.

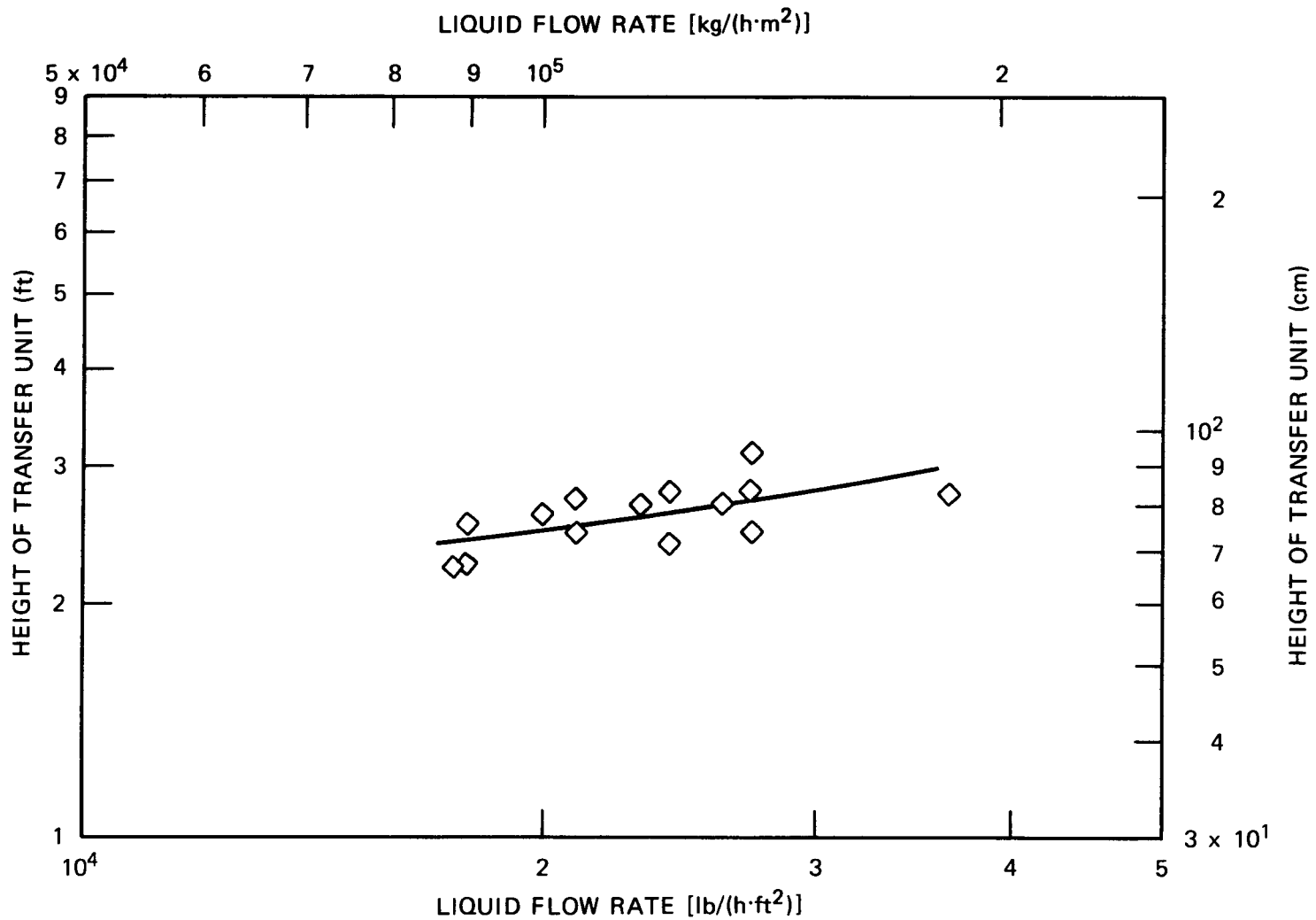


Fig. 8. Effect of liquid flow rate on HTU for 2.54-cm (1-in.) plastic pall ring.

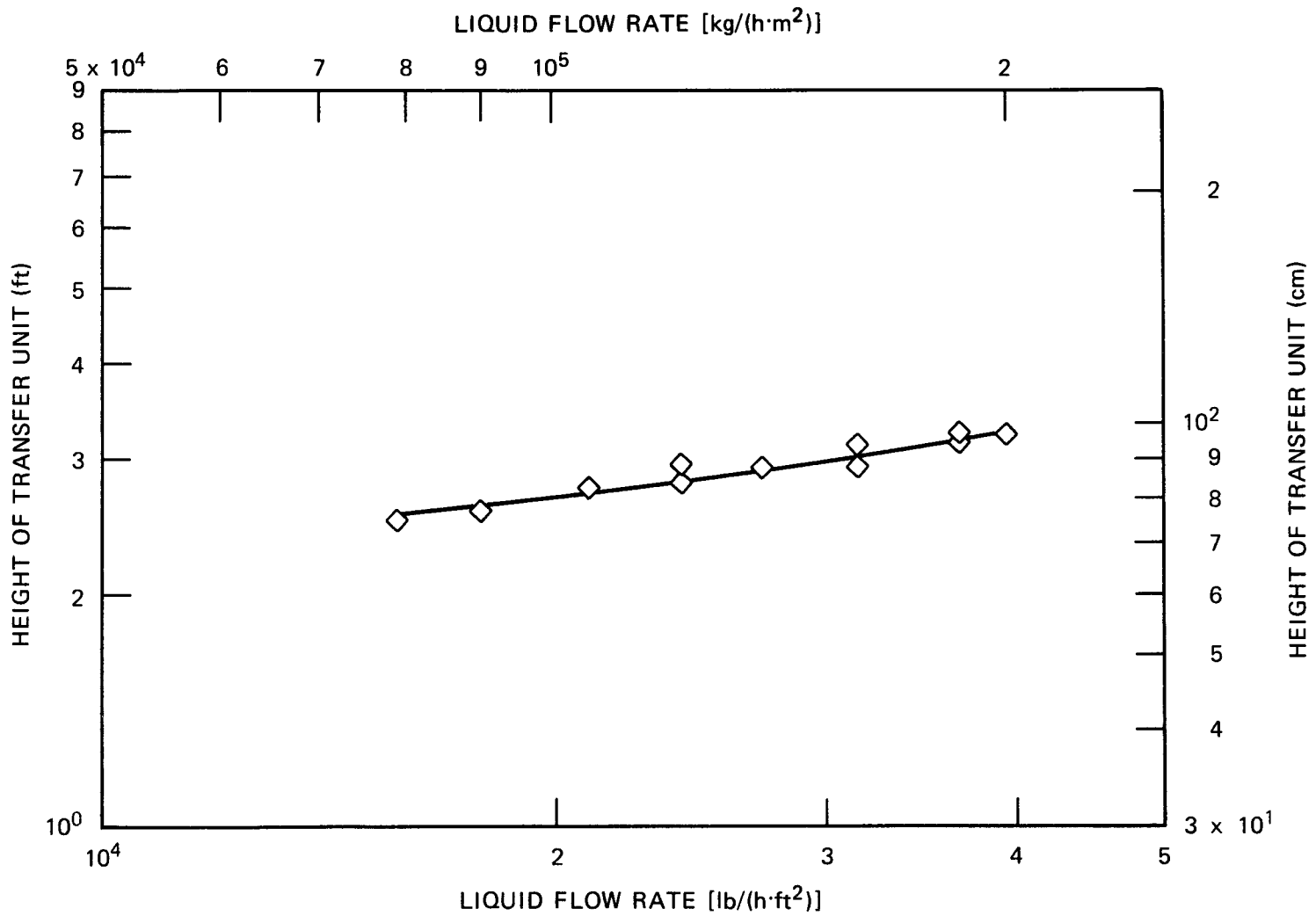


Fig. 9. Effect of liquid flow rate on HTU for 3.81-cm (1.5-in.) plastic pall ring.

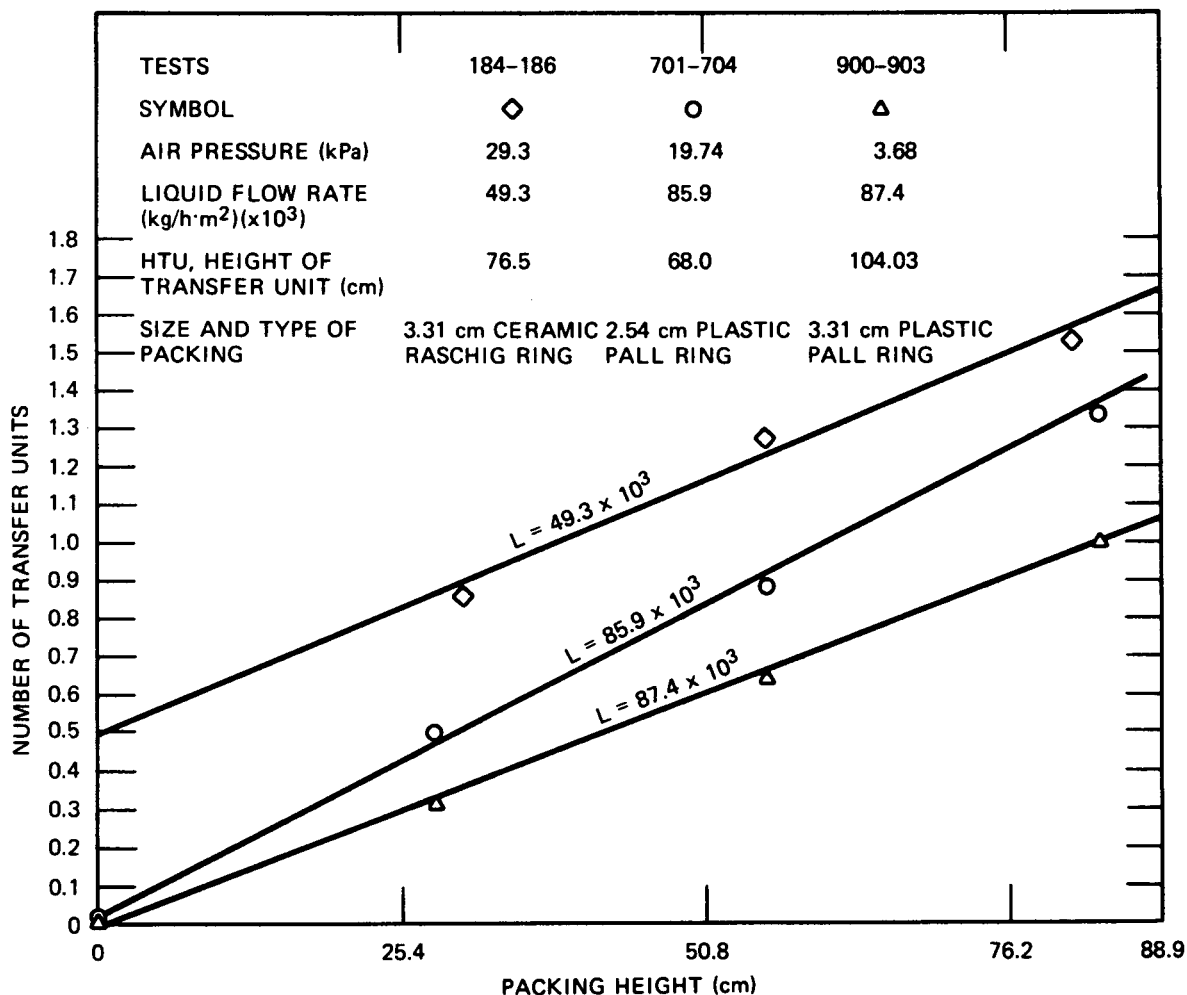


Fig. 10. Relationship between NTU and packing height at different liquid flow rates and packing.

Extrapolating the line (Tests 184 through 186) of Fig. 10 to zero NTU gives the height of additional packing that would be equivalent to the end effect. This line (Tests 184 through 186) is from the first series of the tests in which end effect was a problem. The end effect was minimized in our recent data by placing a partition in the upper portion of the test section and by improving the distributor system so that water comes down through ten 15-cm-long tubes that actually touch the top of the packing. In this case, the liquid flows down without falling through the air at all and spreads out with no splashing.

As described previously, the first series of 110 runs¹ was made under experimental conditions allowing measurement of some desorption in the spray section above the packing and the water line leading to the column. With the revised sampling technique and improvement of the distributor system, the values of the new group are believed to be more representative of the packing efficiency under vacuum desorption of air.

Data from the new group of runs with desorption of air on 2.54- and 3.81-cm plastic pall rings are presented in Figs. 11 and 12. In each case, the data have been corrected to 25°C.

4.2 Correlation of Data

The method of Sherwood and Holloway⁶ on correlation of data in a packed column is adapted in this investigation. They have shown that $K_L a$ and HTU may be expressed as power functions of L for deaeration tests on various packing materials as $K_L a \propto L^{1-n}$ and $(HTU)_L \propto L^n$. The value of n varies with both packing size and type; for the three sizes of rings tested, it is 0.25 for 3.81-cm ceramic Raschig ring, 0.34 for 2.54-cm plastic pall ring, and 0.28 for 3.81-cm plastic pall rings.

The effectiveness of mass transfer can also be correlated to Schmidt number in the following relations:

$$\frac{K_L a}{D} = \alpha (L/\mu)^{1-n} (Sc)^{1-s} , \quad (4)$$

$$HTU = \frac{1}{\alpha} (L/\mu)^n (Sc)^s . \quad (5)$$

These relations are derived from the dimensionless form similar to that used by Gilliland and Sherwood¹² in correlating data on vaporization in a wetted-wall column, but an unknown factor with the dimension of length is omitted in the left-hand side and in the first group on the right-hand side of both equations. Because of this omission, the equations are not dimensionless, and the proportionality constant α may be expected to vary with the nature of the packing material and the units employed.

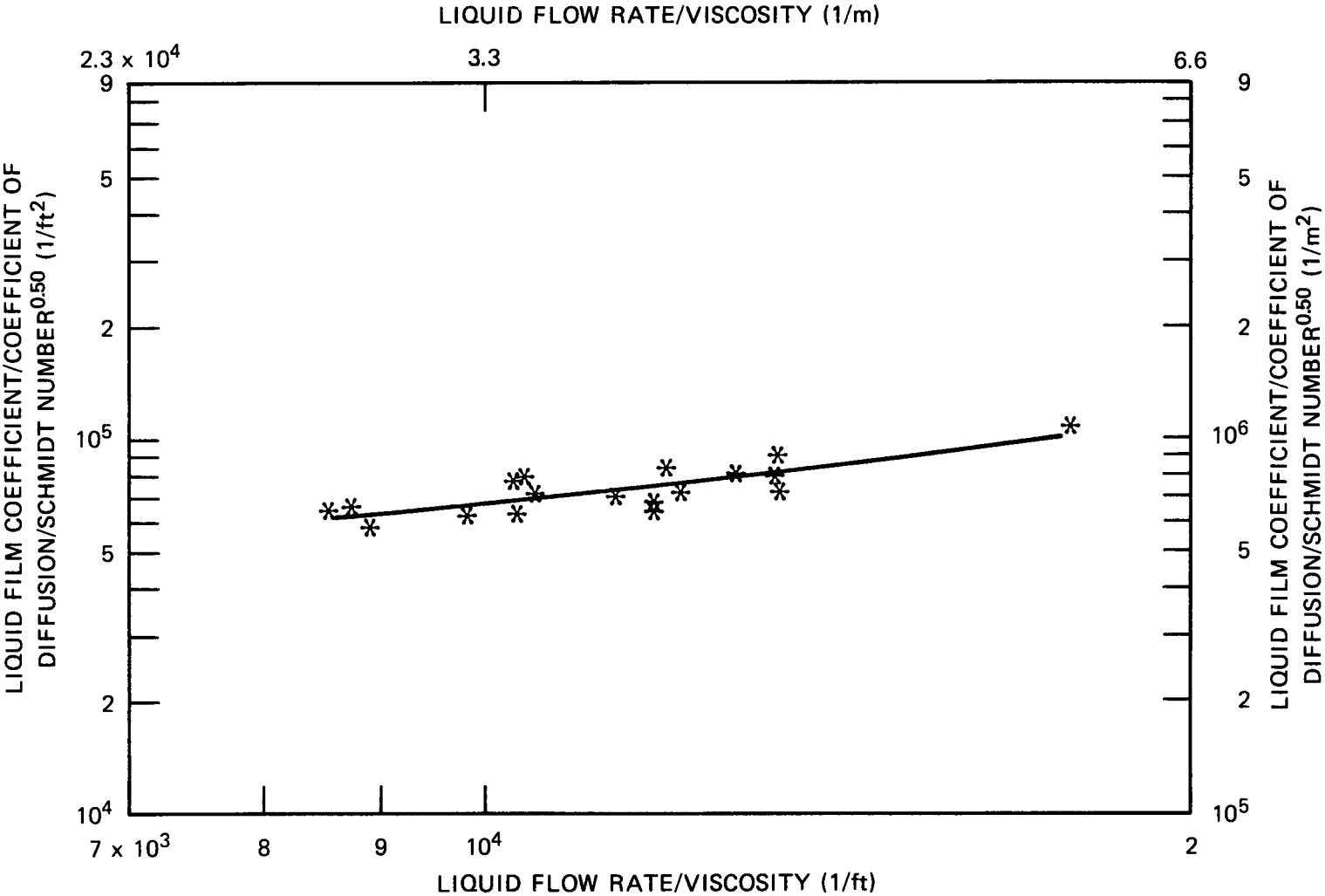


Fig. 11. Co relation of data on vacuum desorption of air in 2.54-cm (1-in.) plastic pall ring.

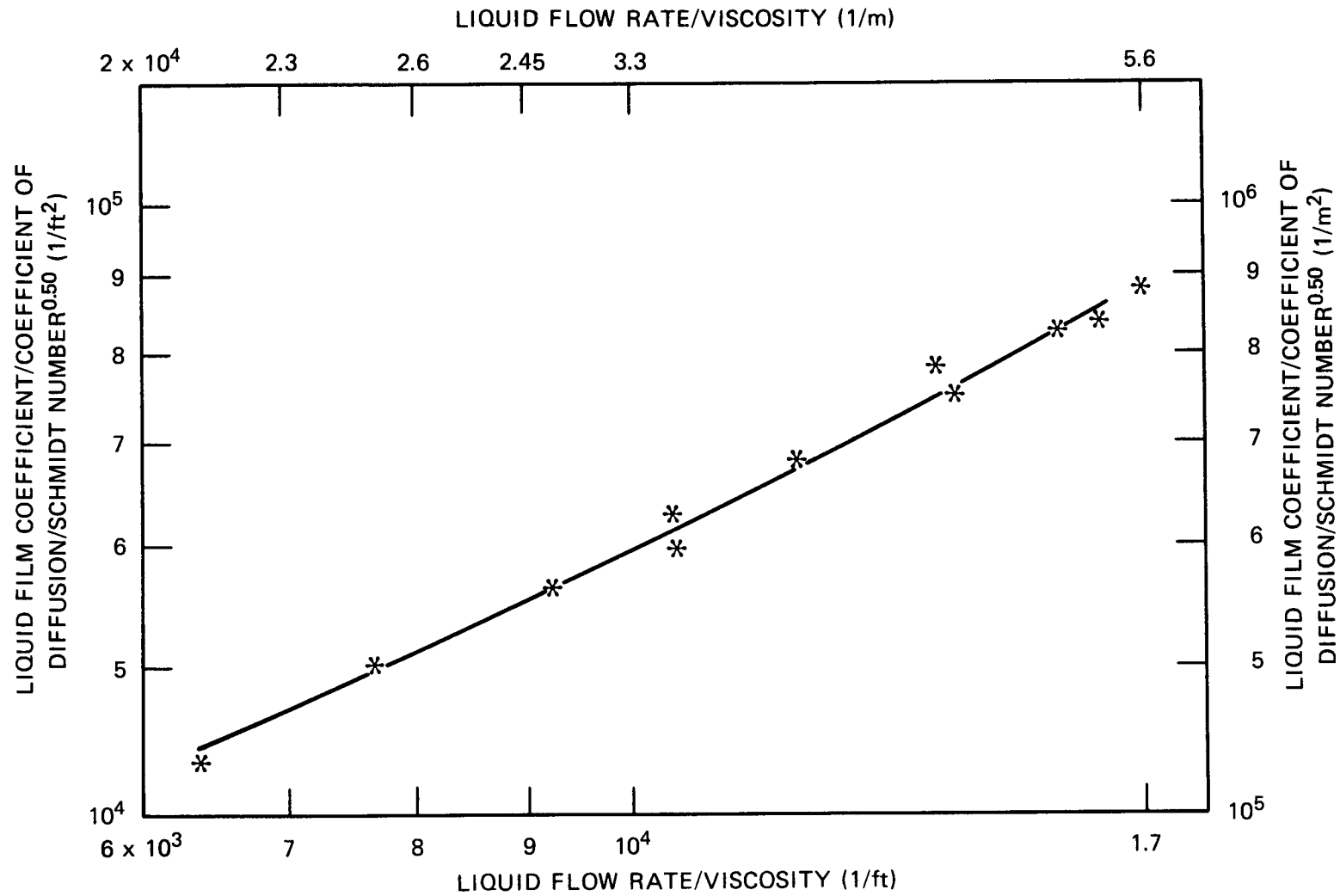


Fig. 12. Correlation of data on vacuum desorption of air in 3.81-cm (1.5-in.) plastic pall ring.

Data from the first series are correlated by a value of 0.50 for s , indicating that $K_L a$ varies as the 0.50 power of the liquid diffusivity for the 3.81-cm ceramic Raschig ring. Sherwood and Holloway⁶ have concluded that for mass transfer in a packed column the s value is 0.50 for all sizes and types of packing. Therefore, Eqs. (4) and (5) would become

$$\frac{K_L a}{D} = \alpha (L/\mu)^{1-n} (Sc)^{0.50}, \quad (6)$$

$$HTU = \frac{1}{\alpha} (L/\mu)^n (Sc)^{0.50}. \quad (7)$$

Table 5 summarizes values of α and n for three packing materials for which data are presented.

Table 5. Values of α and n for three different packings ($s = 0.50$)^a

Packing	α^b	n
3.81-cm ceramic Raschig ring ^c	19.57	0.25
2.54-cm plastic pall ring	113.6	0.34
3.81-cm plastic pall ring	34.86	0.28

^aThe $(1-n)$ values are the slope of lines in Figs. 11 and 12. The α values are the intercept of lines with the x-axis.

^bAll the quantities in Eqs. (6) and (7) must be expressed in $m^3 \cdot kg \cdot h$ units if these values of α are used.

^cData presented in Vol. 1 (Ref.1).

4.3 Maximum Flow of Water Through Packed Column

In the vacuum deaeration, loading is known as the condition where (1) liquid holdup increases rapidly with liquid flow rate, (2) the free area for gas flow becomes smaller, and (3) the pressure drop rises more rapidly. Packed columns are operated best below this loading point.

Flooding and loading velocities in random packings are well correlated by Treybal.¹³ His method is adopted in this investigation to determine the maximum liquid (loading point) flow rates for each type of packing. The corresponding HTU values at a constant liquid flow rate (122,000 kg/h·m²) and at the maximum liquid flow rate are listed in Table 6.

Table 6. Maximum liquid flow rates for different types and sizes of packing

Packing	Size (cm)	Maximum liquid flow, L_{\max} [10^3 kg/(h·m ²)]	HTU (cm)	
			L^a	L_{\max}^b
Ceramic Raschig ring	3.81	122.0	92.0	92.0
	5.08	146.5	72.5 ^c	76.5 ^c
Plastic pall ring	2.54	171.0	80.8	90.2
	3.81	220.0	88.4	103.9
	8.89	293.0	126.5 ^d	133.8 ^d

$$a_L = 122 \times 10^3 \text{ [kg/(h}\cdot\text{m}^2\text{)]}.$$

$$b_L = L_{\max} \text{ [kg/(h}\cdot\text{m}^2\text{)]}.$$

^cThe HTU values presented are from the model of Sherwood and Holloway.

^dThese values are derived from extrapolation by the method shown in the Appendix.

4.4 Results of Deaeration in the Barometric Leg of the Intake System

Vacuum deaeration in a barometric water-intake system requires bubbles to grow in depressurizing flow. The formation of bubble population in a flow field is strongly influenced by the initial nuclei content. Because there is no solid surface other than the pipe wall for vacuum deaeration in a barometric intake pipe, it is hypothesized that the rate of deaeration may be affected by the initial nuclei content in the incoming water as well. The quantitative determination of the concentration and

size distribution of bubble nuclei in the incoming water is beyond the scope of this study but is being studied elsewhere by Hydronautics.¹⁴ However, a qualitative attempt to classify the nuclei content in this study included three cases: low, moderate, and high nuclei concentrations.

In the case of initial low nuclei content, the test water is left overnight to eliminate as many bubble nuclei as possible, and the test loop can only be operated in a once-through mode. In the moderate nuclei content case, aeration is applied only after the barometric intake test in water tank No. 2 (Fig. 3); aeration is applied to both water tank Nos. 1 and 2 in the case of high nuclei content experiments. The vacuum deaeration in a barometric water-intake system was tested in a 5-cm-diam (2-in.) vertical pipe. Water was lifted through the pipe by vacuum pressure.

The water velocity varied from 60 to 180 cm/s. A series of runs for the barometric intake system was completed, and results are presented in Tables 7 through 9. In these runs, the water samples were taken at the

Table 7. Data of barometric system, 8.8-m intake with moderate nuclei^a

TEST	L	TEMP	PAIR	V	XI	XØ	XE	X	RE	NPD
801	28.8	79.6	1.33	3.51	7.98	6.52	.37	18.3	.635E+05	.192E+00
803	28.8	79.2	2.13	2.82	8.00	6.80	.59	15.0	.508E+05	.162E+00
805	28.8	79.1	2.04	3.12	8.11	6.99	.56	13.8	.561E+05	.148E+00
807	28.8	74.9	2.49	2.68	8.29	7.27	.71	12.3	.456E+05	.135E+00
809	28.8	77.1	1.63	3.37	8.14	6.98	.46	14.3	.591E+05	.151E+00
813	28.8	78.1	1.45	3.73	8.10	6.50	.40	19.8	.663E+05	.208E+00
814	28.8	78.1	2.39	2.59	8.10	7.00	.66	13.6	.459E+05	.148E+00
815	28.8	77.8	1.87	3.28	8.10	6.95	.52	14.2	.580E+05	.152E+00
816	28.8	78.7	1.82	3.10	8.22	7.26	.50	11.7	.555E+05	.124E+00
817	28.8	78.8	1.10	3.86	8.32	6.63	.30	20.3	.691E+05	.211E+00
819	28.8	78.9	2.22	2.55	8.24	6.98	.61	15.3	.457E+05	.165E+00

^aVariables are expressed in the following units:

L = ft

Temp = °F

P_{air} = in. Hg

V = ft/s

D = ft²/h

Table 8. Data of barometric intake with no nuclei^a

TEST	L	TEMP	PAIR	V	XI	XØ	XE	Z	RE	NPD
800	28.3	70.4	2.81	3.95	8.00	7.25	.84	9.4	.636E+05	.105E+00
804	28.3	66.1	3.00	4.02	9.29	8.22	.93	11.5	.609E+05	.128E+00
808	28.3	70.2	4.60	2.28	8.78	7.97	1.38	9.2	.367E+05	.109E+00
720	28.3	70.0	2.33	3.13	8.03	7.50	.70	6.6	.502E+05	.723E-01
727	28.3	71.1	4.43	2.90	8.32	7.80	1.31	6.3	.471E+05	.742E-01
728	28.3	71.4	3.43	2.37	8.32	7.69	1.01	7.6	.386E+05	.862E-01
731	28.3	71.7	.82	5.85	8.30	7.25	.24	12.7	.956E+05	.130E+00
732	28.3	72.1	2.48	3.75	8.30	7.53	.73	9.3	.616E+05	.102E+00
733	28.3	73.8	1.16	5.10	8.41	6.90	.34	18.0	.856E+05	.187E+00
734	28.3	73.6	1.86	3.35	8.41	7.10	.54	15.6	.561E+05	.166E+00
735	28.3	72.1	3.02	3.95	8.20	7.50	.89	8.5	.649E+05	.957E-01
739	28.3	74.9	3.67	3.02	8.12	7.49	1.05	7.8	.514E+05	.891E-01
747	28.3	75.7	2.33	4.02	8.10	7.20	.66	11.1	.691E+05	.121E+00

^aVariables are expressed in the following units:

L = ft

Temp = °F

P_{air} = in. Hg

V = ft/s

D = ft²/h

entrance to the barometric leg and again at the end of barometric intake. Tables 7 and 9 are for the condition of moderate nuclei when the intake heights are 8.8 and 7.8 m, respectively. Table 8 shows the results of barometric intake when few nuclei exist in the water. In this case, water remains overnight in the tank undisturbed.

The barometric intake system deaeration is presented according to the following equations:

$$PDA = a(v)^b, \quad (8)$$

$$NPD = c(v)^d, \quad (9)$$

$$NPD = e(Re)^f. \quad (10)$$

Table 10 summarizes values a through f for various intake heights and amounts of nuclei. The percentage of deaeration (PDA) and normalized percentage deaeration (NPD) vs water velocity (V) and Reynolds number (Re) are shown in Figs. 13 through 22.

Table 9. Data of barometric system 7.8-m intake
with moderate nuclei^a

TEST	L	TEMP	PAIR	V	XI	XØ	XE	Z	RE	NPD
711	25.5	74.2	1.69	5.48	8.45	7.59	.49	10.2	.925E+05	.108E+00
712	25.5	78.3	4.47	2.49	7.80	7.10	1.24	9.0	.443E+05	.107E+00
713	25.5	78.5	4.29	2.90	7.71	7.28	1.19	5.6	.518E+05	.659E-01
714	25.5	78.1	3.87	3.38	7.78	7.17	1.08	7.8	.600E+05	.910E-01
715	25.5	77.1	3.12	4.14	7.80	6.95	.87	10.9	.725E+05	.123E+00
716	25.5	78.7	2.25	4.91	7.65	6.90	.62	9.8	.878E+05	.107E+00
717	25.5	78.6	1.27	5.46	7.70	6.50	.35	15.6	.976E+05	.163E+00
718	25.5	78.9	1.74	5.15	7.60	6.70	.48	11.8	.924E+05	.126E+00
721	25.5	76.5	3.13	3.73	8.25	7.42	.88	10.1	.649E+05	.113E+00
722	25.5	77.1	1.75	4.61	8.18	7.50	.49	8.3	.807E+05	.885E-01
723	25.5	77.2	5.05	2.38	8.20	7.63	1.42	7.0	.418E+05	.840E-01
724	25.5	77.9	4.59	3.12	8.12	7.50	1.28	7.6	.553E+05	.906E-01
725	25.5	77.6	3.56	4.14	8.10	7.45	.99	8.0	.730E+05	.915E-01
729	25.5	77.6	1.09	5.91	8.30	7.10	.31	14.5	.104E+06	.150E+00
730	25.5	77.9	2.41	5.13	8.40	7.40	.67	11.9	.909E+05	.129E+00
736	25.5	75.4	4.78	2.45	8.24	7.60	1.36	7.8	.419E+05	.930E-01
737	25.5	75.8	4.53	3.38	8.22	7.63	1.29	7.2	.581E+05	.851E-01
740	25.5	78.4	2.74	4.29	7.97	7.35	.76	7.8	.765E+05	.860E-01
741	25.5	78.4	2.02	4.98	8.16	7.10	.56	13.0	.888E+05	.139E+00
742	25.5	78.8	1.48	5.54	8.00	6.79	.41	15.1	.993E+05	.159E+00
744	25.5	77.9	1.45	5.64	8.19	7.28	.40	11.1	.998E+05	.117E+00
745	25.5	78.1	2.20	5.23	8.15	7.31	.61	10.3	.928E+05	.111E+00
746	25.5	78.3	2.83	4.56	8.21	7.39	.78	10.0	.813E+05	.110E+00
748	25.5	77.2	3.70	3.79	8.20	7.60	1.04	7.3	.666E+05	.838E-01
749	25.5	77.4	4.13	3.34	8.05	7.45	1.15	7.5	.587E+05	.870E-01
750	25.5	77.4	4.59	2.82	8.05	7.35	1.28	8.7	.496E+05	.103E+00

^aVariables are expressed in the following units:

L = ft

Temp = °F

P_{air} = in. Hg

V = ft/s

D = ft²/h

Table 10. Empirical values for barometric intake system^a

Intake system	Variables					
	a	b	c	d	e	f
7.8 m and moderate nuclei	0.340	0.691	0.843	0.525	0.03	0.523
8.8 m and moderate nuclei	0.314	0.85	0.552	0.74	0.0048	0.74
Variable height with no nuclei	0.325	0.727	0.662	0.597	0.015	0.599
8.4 m and high nuclei	0.027	1.33			0.067	0.26

^aEqs. (8) through (10).

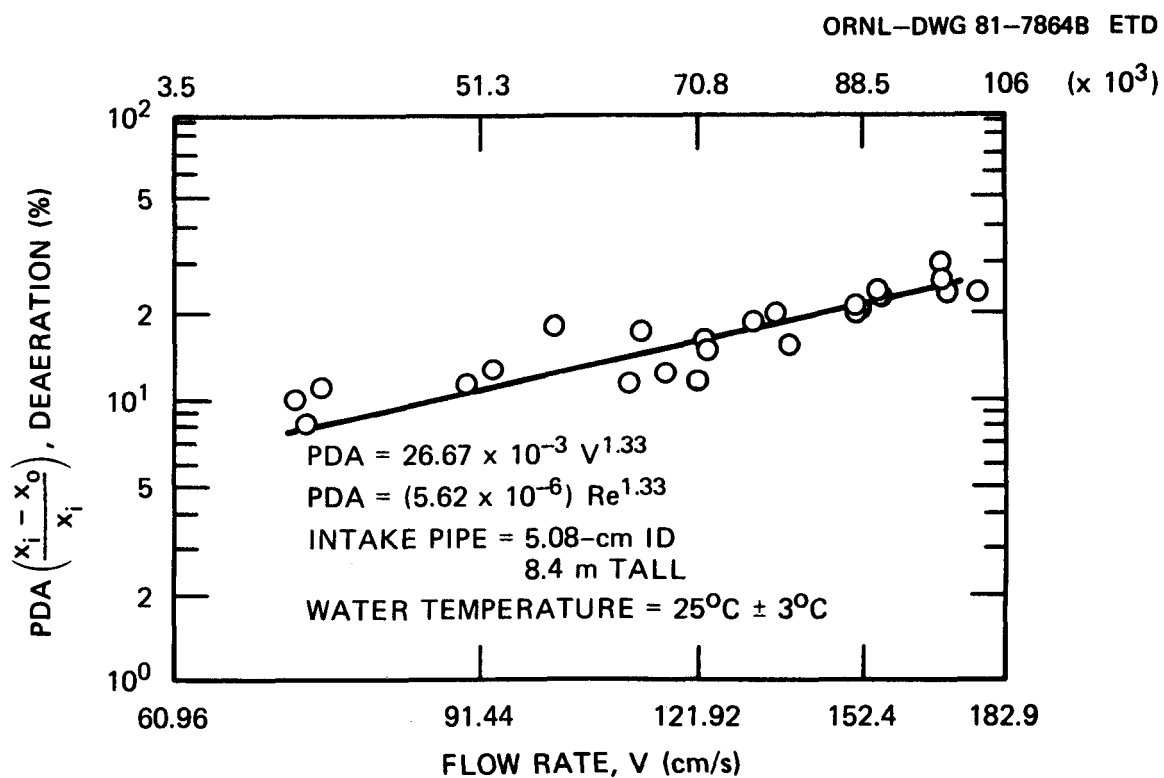


Fig. 13. OTEC barometric intake configuration.

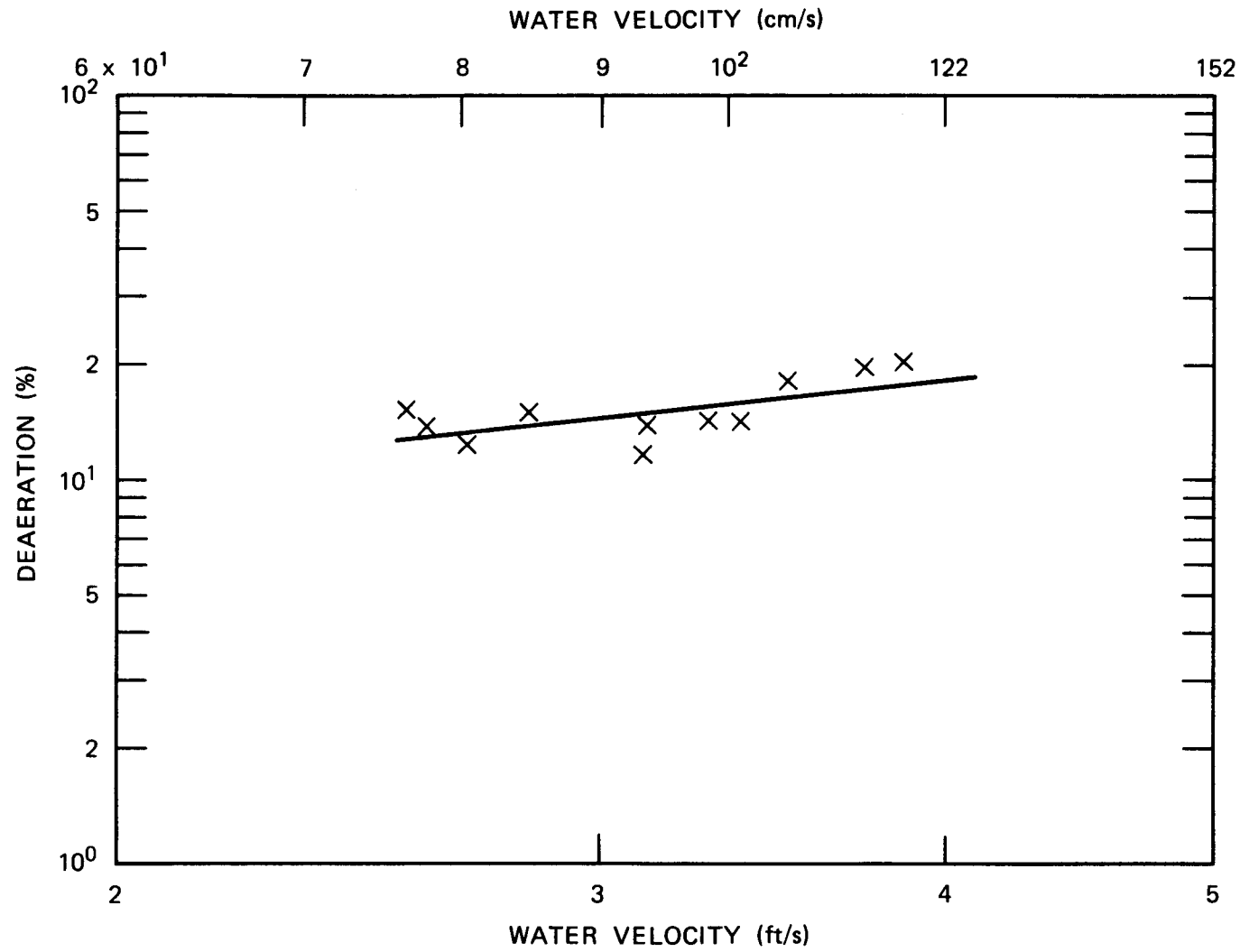


Fig. 14. Percentage deaeraton in 8.8-m intake system with moderate nuclei.

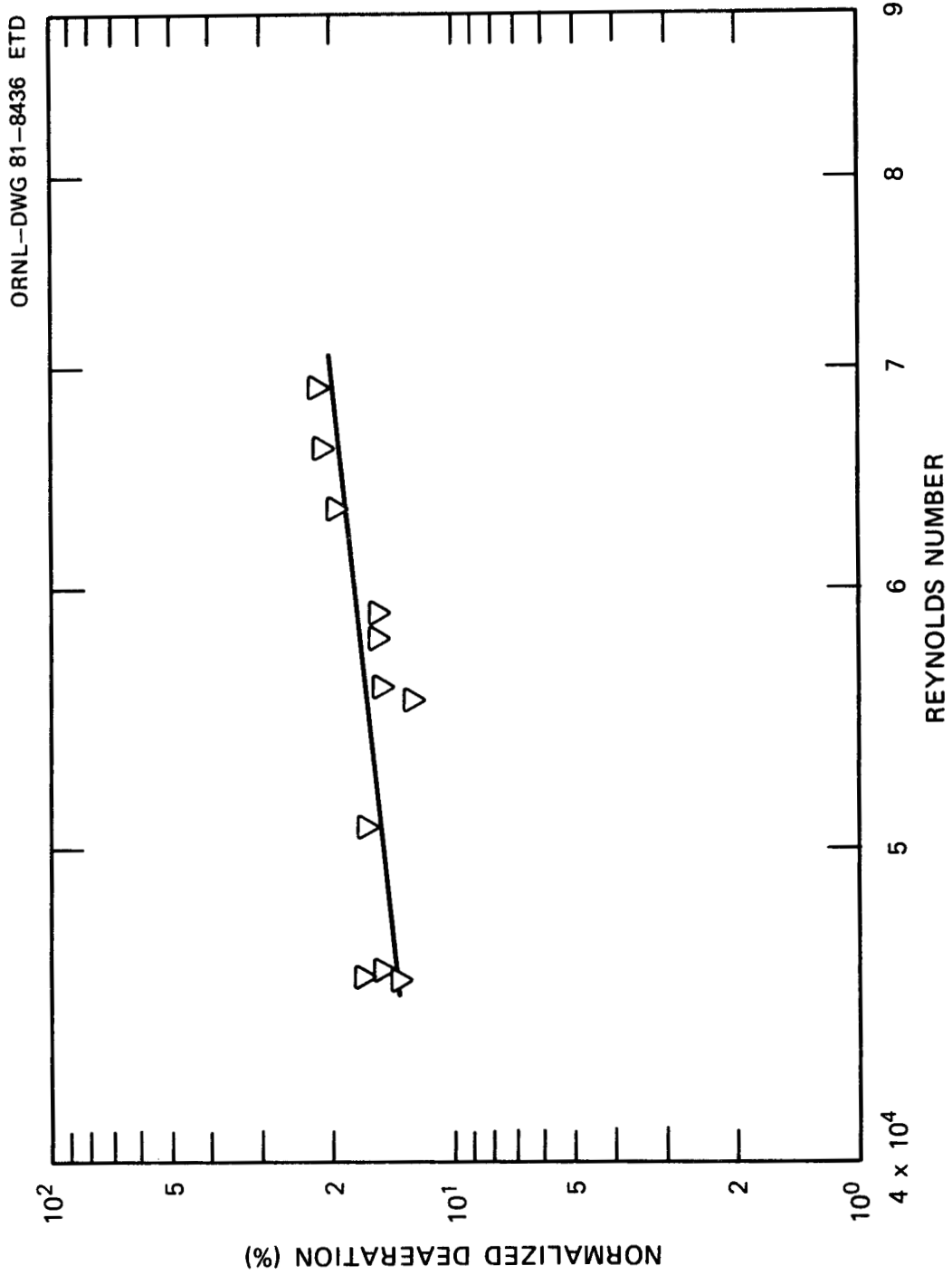


Fig. 15. Normalized deaeration in 8.8-m intake system with moderate nuclei.

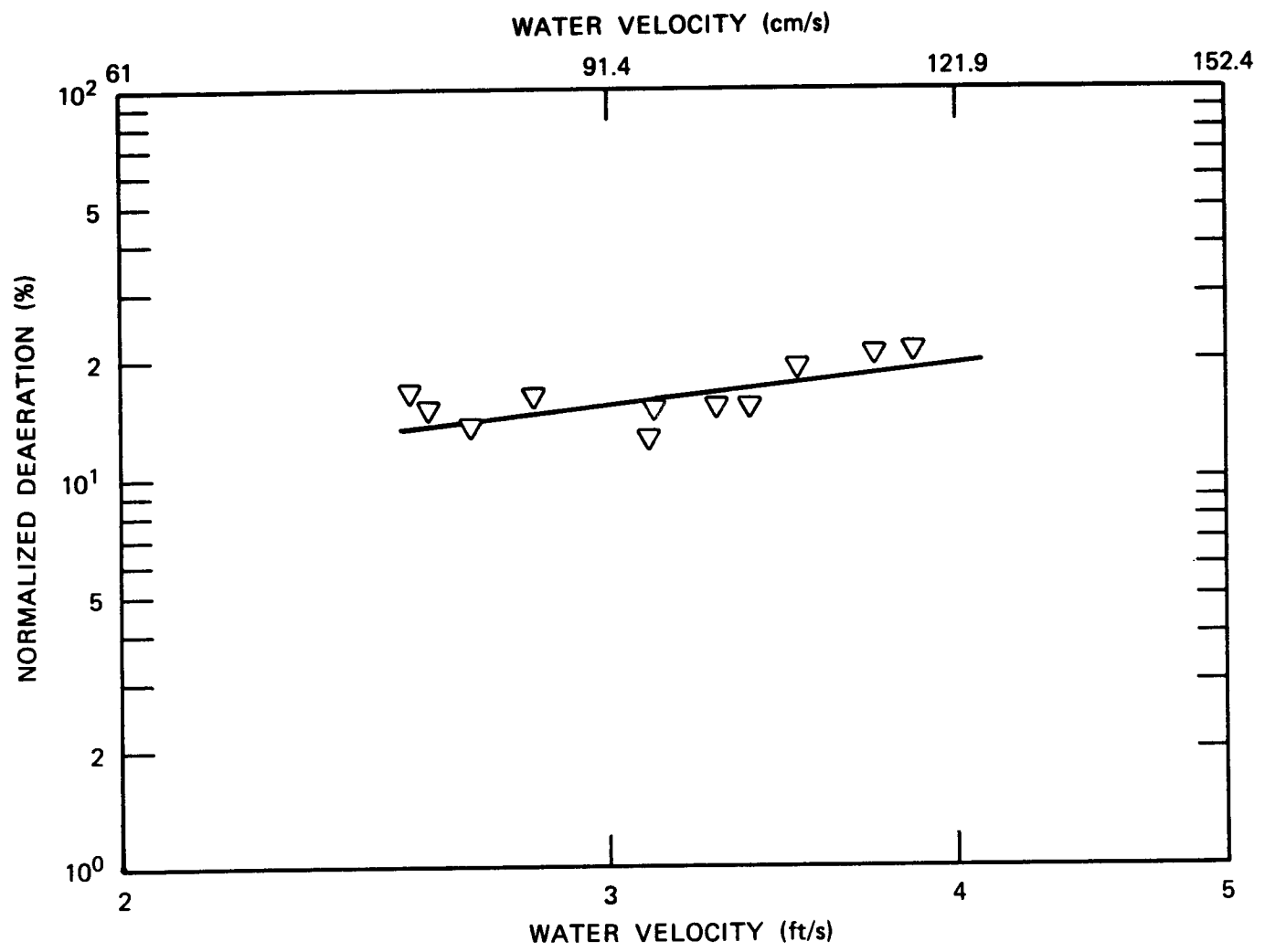


Fig. 16. Variation of normalized deaeration with water velocity in 8.8-m intake system with moderate nuclei.

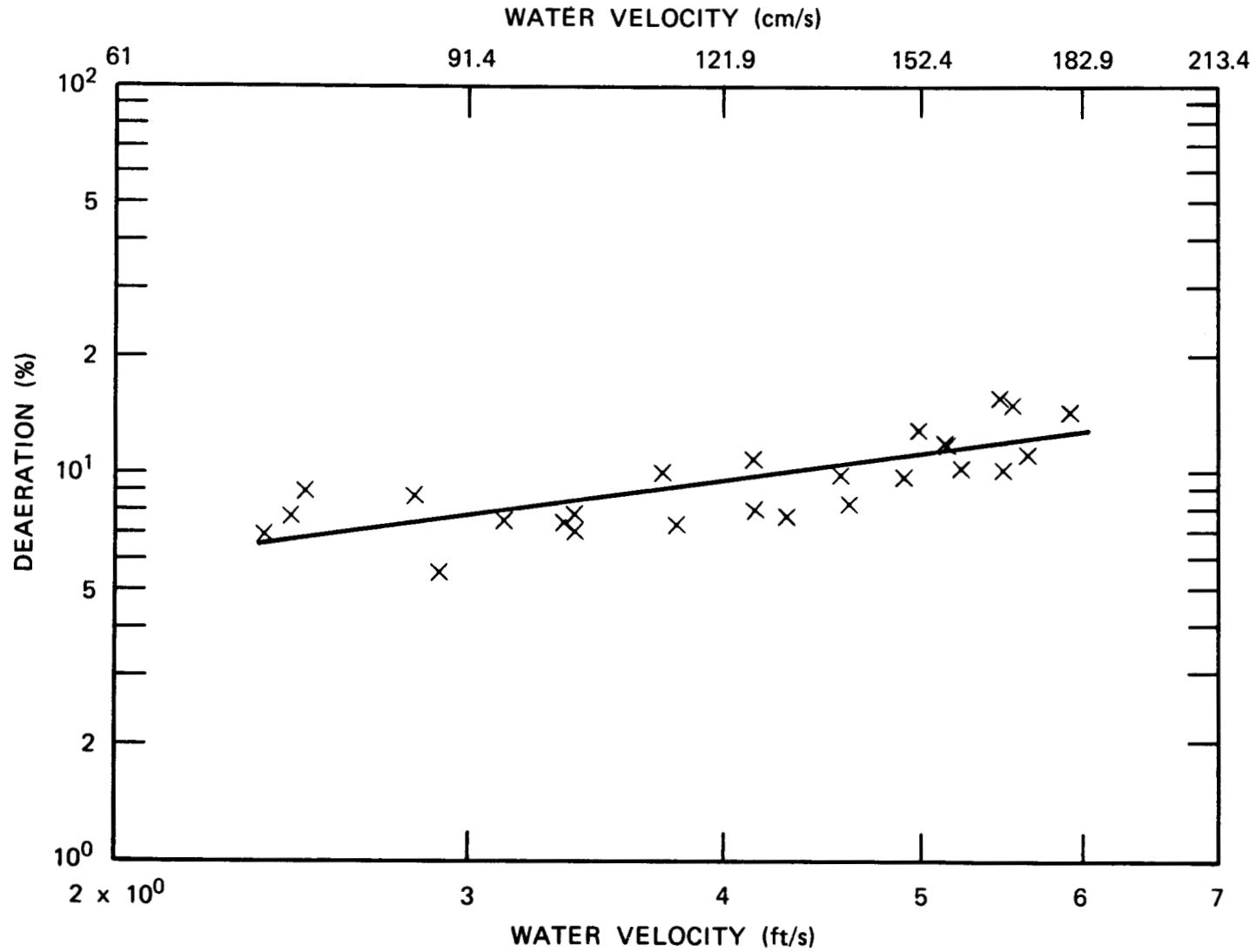


Fig. 17. Variation of percentage deaeration with water velocity in 7.8-m intake system with moderate nuclei.

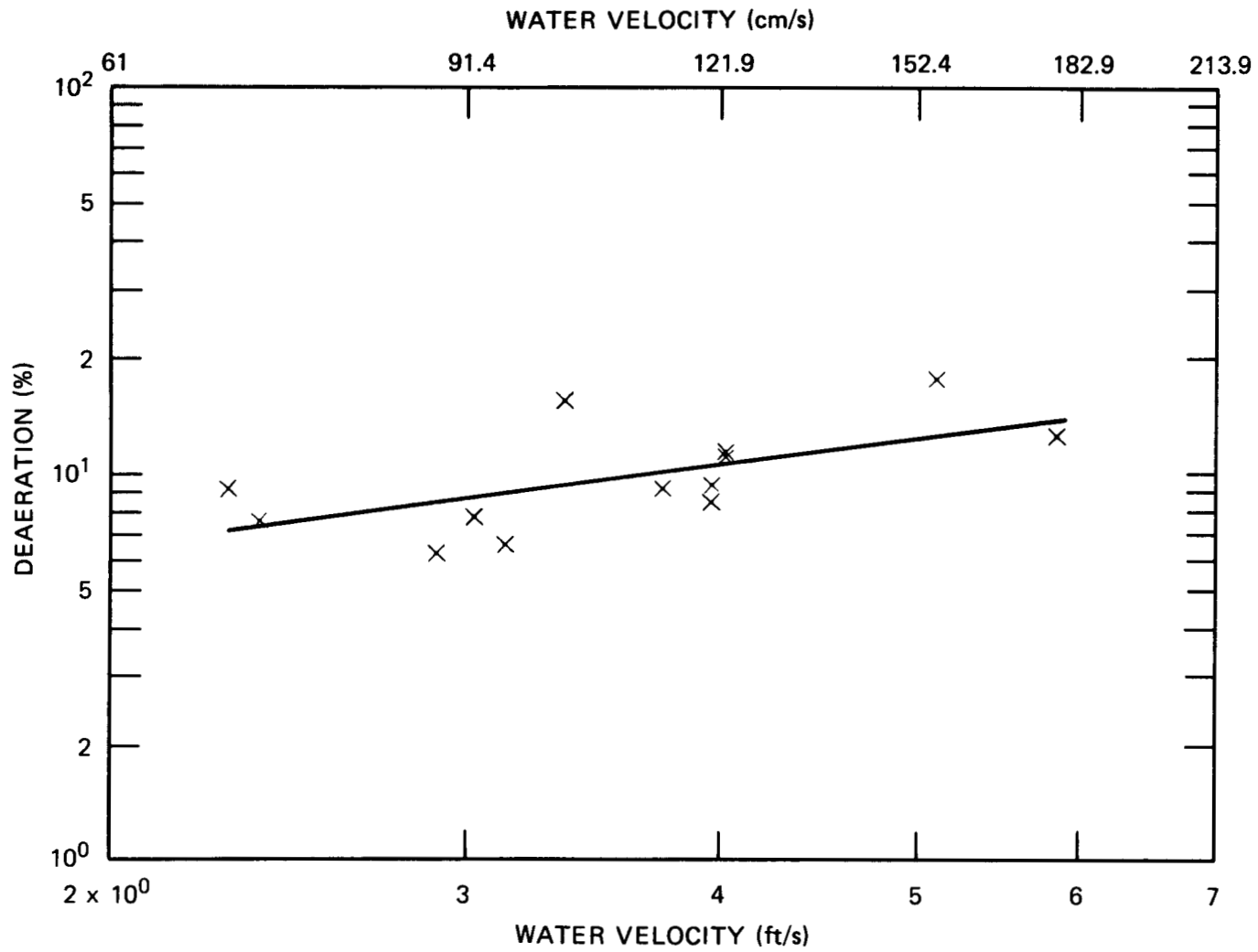


Fig. 18. Variation of percentage deaeration with water velocity for barometric intake with no nuclei.

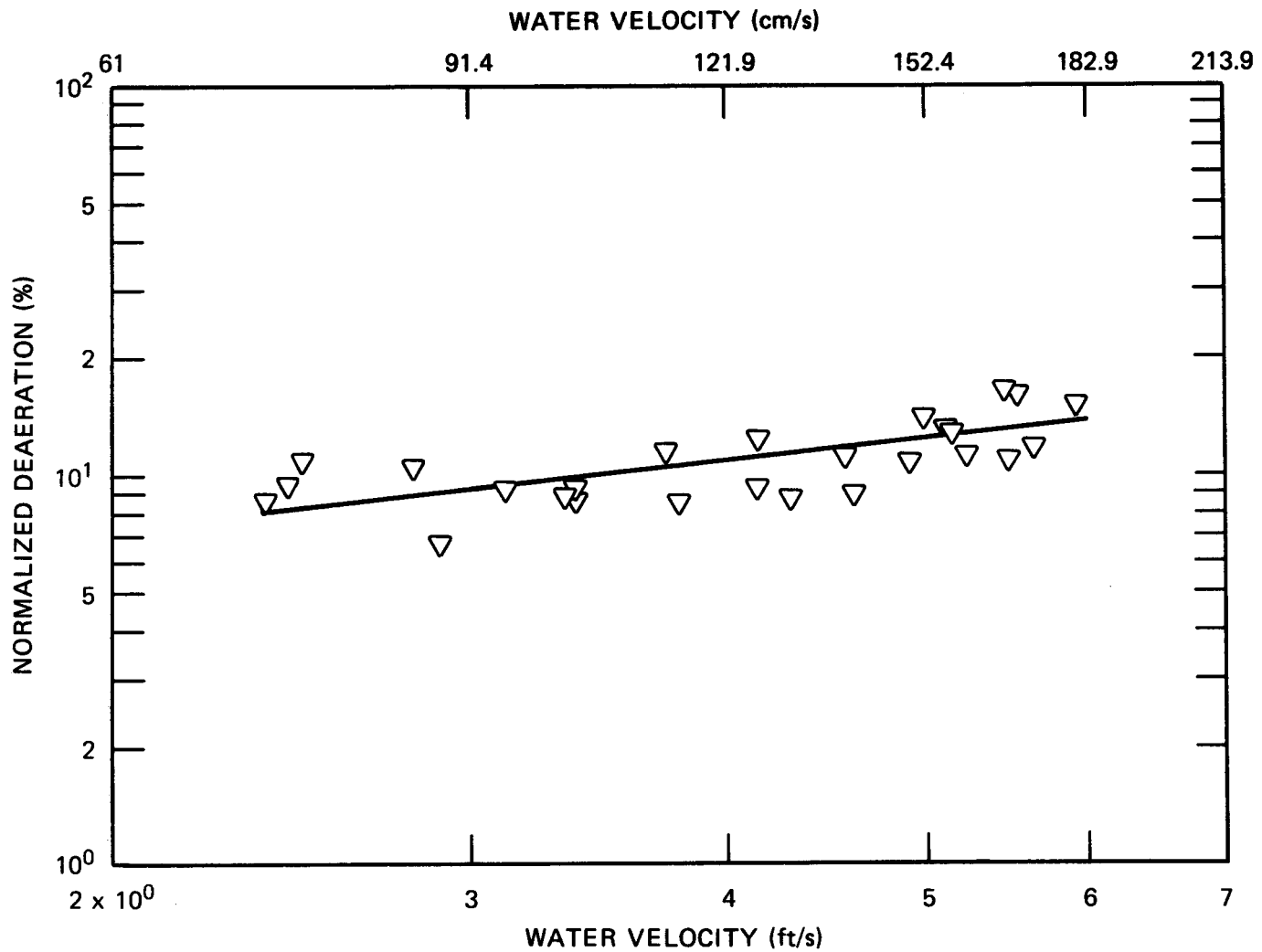


Fig. 19. Variation of normalized deaeration with water velocity in 7.8-m intake system with moderate nuclei.

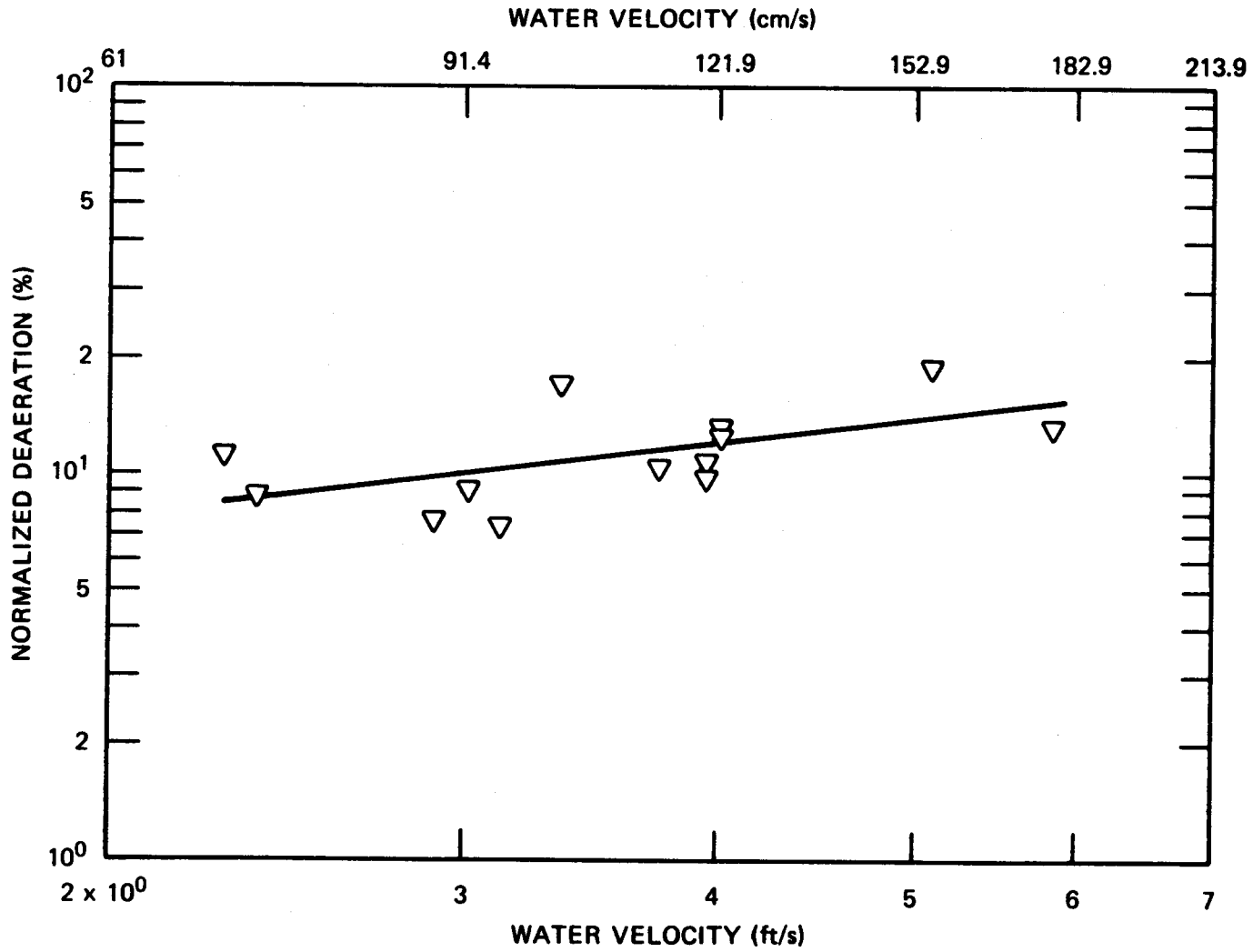


Fig. 20. Variation of normalized deaeration with water velocity for barometric intake with no nuclei.

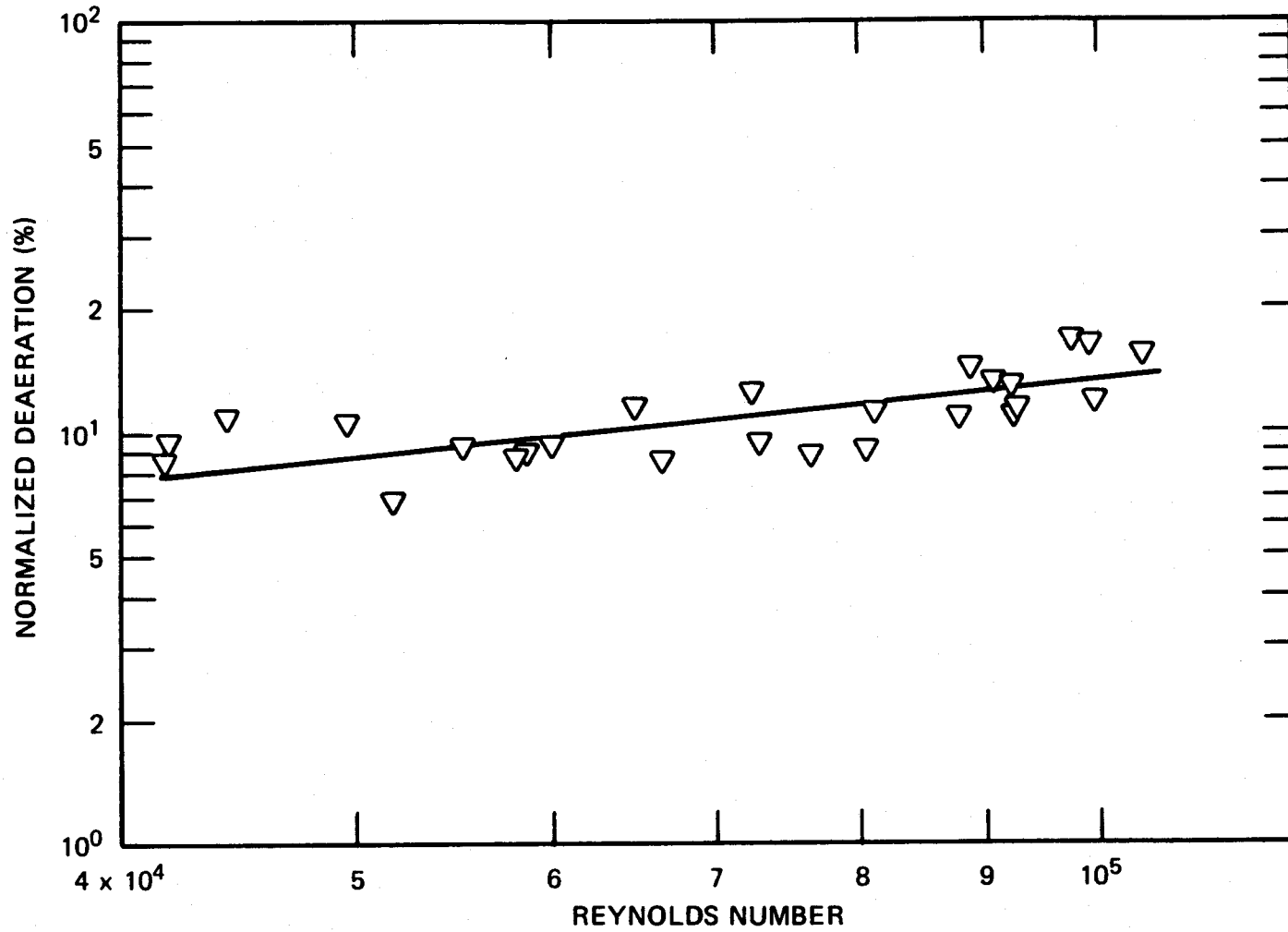


Fig. 21. Variation of normalized deaeration with Reynolds number for 7.8-m intake system with moderate nuclei.

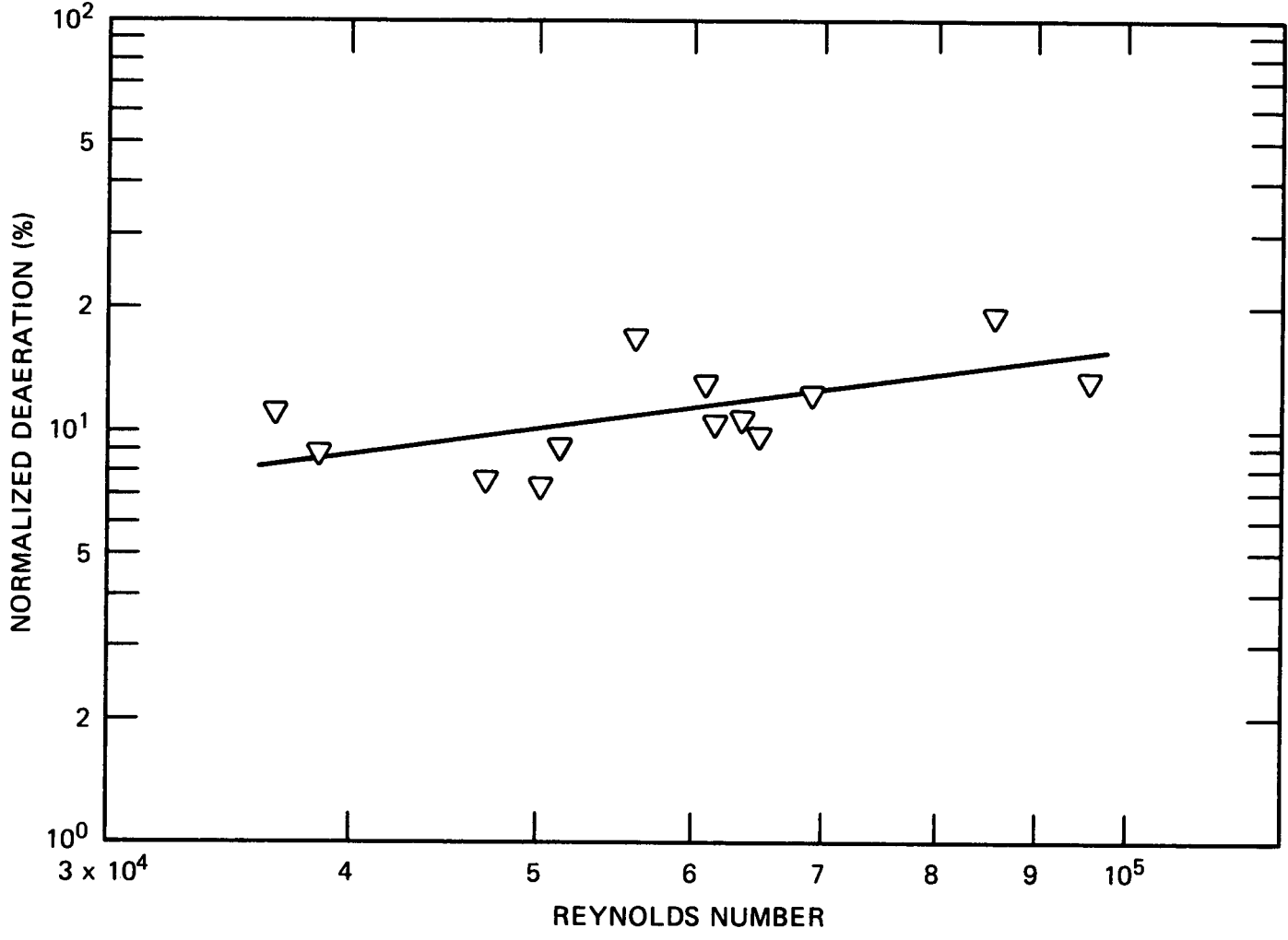


Fig. 22. Variation of normalized deaeration with Reynolds number for barometric intake with no nuclei.

4.5 Application to OTEC Open-Cycle Plant and Economic Evaluation

The experimental results and derived data from the gas absorption tests were applied to the Westinghouse deaerator subsystem design¹⁵ to compute the deaerator cost and the pumping power for various packings.

The deaerator cost is based on the following:

z = cost of packing, \$353/m³ for ceramic Raschig rings and \$141/m³ for plastic pall rings;

x = cost of packing support plates, \$215.30/m²;

y = cost of liquid distributors, \$269.10/m².

The cost of the deaerator enclosure is not included in this summation because it is considered to be part of the hull. Evidently, larger liquid flow rates yield a lower-cost deaerator because the variation of the HTU with liquid rate is small in the range tested.

The cost of the column internal derived by Westinghouse¹⁵ is represented as

$$\text{cost} = \left\{ \left[x + y + z \left(\frac{\text{HTU}}{100} \right) \ln(1 - \epsilon)^{-1} \right] / L_{\text{max}} \right\} W_{\text{hsw}}, \quad (11)$$

where

ϵ = stage efficiency,

W_{hsw} = warm seawater flow, kg/h,

L_{max} = maximum liquid flow rate for a given packing,

HTU = height of transfer unit, cm.

The items that contribute to the total deaerator height and the magnitude of each contribution are given in the Westinghouse study.¹⁵ The height of major deaerator components excluding the packing height is 147.2 cm; this value is a realistic estimate.

The total height in centimeters of the packed column is then

$$h = 147.2 + h_1, \quad (12)$$

where the height of packing is

$$h_1 = (\text{HTU})(\text{NTU}) = \text{HTU} \ln \left(\frac{1}{1 - \epsilon} \right). \quad (13)$$

Therefore, Eq. (12) can be expressed as

$$h = 147.2 - [(\text{HTU}) \ln(1 - \epsilon)]. \quad (14)$$

The pumping power in megawatts is

$$\text{MW} = \frac{W_{\text{hsw}} h}{36.65 \times 10^9 \eta} = \frac{W_{\text{hsw}}}{36.65 \eta} \times [147.2 + (\text{HTU}) \ln(1 - \epsilon)^{-1}]. \quad (15)$$

The pump combined efficiency was assumed to be 0.715.

Results of deaeration cost and the pumping power for various packings and for the barometric intake system (8.4-m height intake) are tabulated in Table 11. Results are shown for the condition of 455×10^6 kg/h of warm (27°C) seawater.

Table 11. Deaerator cost and pumping power for various packings and for barometric intake system^a

Packing	Size (cm)	Barometric intake deaeration effect			
		Without		With	
		Deaerator cost (\$ × 10 ⁶)	Pumping power (MW)	Deaerator cost (\$ × 10 ⁶)	Pumping power (MW)
Ceramic Raschig ring	3.81	2.58	5.10	2.40	4.57
	5.10	2.85	4.68	2.56	4.23
Plastic pall ring	3.81	1.50	5.43	1.38	4.83
	8.90	1.22	6.26	1.12	5.49

^aWarm seawater flow rate = 455×10^6 kg/h; deaerator effectiveness = 0.80.

Results indicate that use of the larger plastic pall ring has a very favorable impact on the cost, but the power consumption is increased somewhat.

The deaerator cost estimates and the pumping power needs for barometric intake and a deaerator packed with different types and sizes of packing were computed according to Eqs. (8), (11), and (15) and are listed in Table 11.

5. CONCLUSIONS

The following conclusions were drawn from the experimental study for vacuum deaeration in a packed column and in a barometric intake configuration:

1. Vacuum deaeration HTU information for two sizes of plastic pall rings was obtained because there was no mass-transfer/HTU information in the literature for the plastic pall rings.
2. We found that deaeration occurs in barometric intake to a packed column. In the system tested, deaeration of up to 27% was found for a water flow rate of 1.8 m/s with high nuclei content. The barometric intake will have the advantage of achieving a partial predeaeration and thus reduce the cost of a full deaeration system. Deaeration in a barometric intake may be affected by physical parameters such as water flow rate, the existence of nuclei in the water, and the vacuum pressure.
3. Our study indicates that with the barometric intake deaeration effect, ~10% reductions both in cost and pumping power can be achieved when barometric intake is combined with the packed column.

REFERENCES

1. A. Golshani and F. C. Chen, *OTEC Gas Desorption Studies*, ORNL/TM-7438/V1 (October 1980).
2. G. Claude, "Power from Tropical Seas," *Mech. Eng.* 52, 1039 (December 1930).
3. J. T. Lewis and W. G. Whitman, "Principles of Gas Absorption," *Ind. Eng. Chem.* XVI, 1215 (1924).
4. R. Higbie, "The Rate of Absorption of a Pure Gas into a Liquid During Short Period of Exposure," *Trans. Am. Inst. Chem. Eng.* 3, 365 (1935).
5. P. V. Danckwerts, "Significance of Liquid-Film Coefficients in Gas Absorption," *Ind. Eng. Chem.* 43, 1460 (1951).
6. T. K. Sherwood and A. L. Holloway, "Performance of Packed Towers Liquid Film Data for Several Packings," *Trans. Am. Inst. Chem. Eng.* 36, 39 (1940).
7. E. L. Knoedler and C. F. Bonilla, "Vacuum Degasification of Water in a Packed Column," *Chem. Eng. Prog.* 50(3), 125-133 (1954).
8. J. T. Chambers, *Sea Water Conversion*, Institute of Engineering Research, University of California, Berkeley, Series 75, Issue No. 16, Sept. 3, 1959.
9. D. M. Eissenberg, *Summary of Present Status for Design and Analysis of Vacuum Deaerators for Distillation Plants*, Office of Saline Water, ORNL/TM-3454 (April 1972).
10. E. A. Rasquin, G. Lynn, and D. N. Hanson, "Vacuum Degassing of Carbon Dioxide and Oxygen from Water in Packed Columns," *Ind. Eng. Chem., Fundam.* 16(1), 170-174 (1977).
11. P. Marchand, "Recent French OTEC Work in the Area of OTEC Systems," 7th Ocean Energy Conference, Washington, D.C., June 1980.
12. E. R. Gilliland and T. K. Sherwood, "Diffusion of Vapors Into Air Steams," *Ind. Eng. Chem.* 26, 516 (1934).
13. R. E. Treybal, *Mass Transfer Operations*, pp. 159-163, McGraw-Hill, New York, 1968.
14. W. T. Lindenmuth, and H. L. Liu, Hydronautics Inc., personal communication to A. Goshani, Oak Ridge National Laboratory, February 1981.
15. Westinghouse Electric Corp., *100 MWe OTEC Alternate Power Systems*, Final Report, DOE Contract EG-77-C-05-1473 (March 1979).



Appendix

ESTIMATED VALUE OF HTU FOR 8.89-cm (3.5-in.)
PLASTIC PALL RING

As explained earlier, the ratio of the column diameter to packing dimension should be at least 8:1. Because the diameter of the column being investigated is 30.48 cm, 8.89-cm plastic pall rings could not be used. Therefore, experimentally obtained data were extrapolated to estimate the HTU for 8.89-cm pall rings.

The Sherwood and Holloway HTU values for various sizes of ceramic Raschig rings and different liquid flow rates in kilograms per hour per square meter are given in Table A.1. The ratio of one HTU value to the prior value is 1.11 (Table A.1). Therefore, this table can be extrapolated further by multiplying the last HTU value by 1.11, thus yielding the next HTU value when the ring size is incremented by 1.27 cm. This same method has been used to extrapolate for plastic pall rings. Table A.2 shows experimentally determined HTU values for two ring sizes and flow rates.

The HTU ratio for the plastic pall rings at a flow rate of 9.76×10^4 kg/h·m² is 1.105, and the HTU ratio at a flow rate of 1.71×10^5 kg/h·m² is 1.075. Using these values, the HTU for an 8.89-cm plastic pall ring can be extrapolated as shown in Table A.3.

HTUs can be defined by the following equation:

$$\text{HTU} = a(L)^b, \quad (\text{A.1})$$

where a and b are changing with each ring and L is the liquid flow rate. Consider the condition of the 8.89-cm pall ring in Table A.3:

$$\begin{array}{ll} L = 9.76 \times 10^4 & \text{HTU} = 123.6 \\ L = 1.71 \times 10^5 & \text{HTU} = 129.54 \end{array}$$

Substituting these values into Eq. (A.1) yields the following simultaneous equations:

$$\begin{array}{l} 123.6 = a(9.76 \times 10^4)^b \\ 129.54 = a(1.71 \times 10^5)^b \end{array}$$

Table A.1. HTU values for various sizes of ceramic Raschig ring

Ring sizes (cm)	HTU ^a (cm)	Ratio of HTU ₂ /HTU ₁	HTU ^b (cm)	Ratio of HTU ₂ /HTU ₁
2.54	35.11		41.48	
3.81	39.01	1.11	46.02	1.11
5.08	43.29	1.11	51.22	1.11

$$a_L = 85.4 \times 10^3 \text{ kg/h}\cdot\text{m}^2.$$

$$b_L = 17.9 \times 10^4 \text{ kg/h}\cdot\text{m}^2.$$

Table A.2. HTU values for plastic pall ring

Ring sizes (cm)	HTU ^a (cm)	Ratio of HTU ₂ /HTU ₁ ^a	HTU ^b (cm)	Ratio of HTU ₂ /HTU ₁ ^b
2.54	75		90.22	
3.81	82.91	1.105	97.0	1.105

$$a_L = 9.76 \times 10^4 \text{ kg/h}\cdot\text{m}^2.$$

$$b_L = 1.71 \times 10^5 \text{ kg/h}\cdot\text{m}^2.$$

Table A.3. HTU values for plastic pall ring obtained by extrapolation method

Ring sizes (cm)	HTU ^a (cm)	HTU ^b (cm)
5.08	91.62	104.27
6.35	101.23	112.1
7.62	111.9	120.5
8.89	123.6	129.54

$$a_L = 9.76 \times 10^4 \text{ kg/h}\cdot\text{m}^2.$$

$$b_L = 1.71 \times 10^5 \text{ kg/h}\cdot\text{m}^2.$$

Solving this system of equations yields $a = 47.08$ and $b = 0.084$, giving the following equation for 8.89-cm plastic pall rings:

$$\text{HTU} = 47.08(L)^{0.084} . \quad (\text{A.2})$$

Substituting a flow rate of $2.93 \times 10^5 \text{ kg/h}\cdot\text{m}^2$ into Eq. (A.2) gives an HTU of 135.5 cm.



INTERNAL DISTRIBUTION

- | | | | |
|--------|---------------------|--------|-------------------------------|
| 1. | W. R. Carver | 26. | M. P. Ternes |
| 2-6. | F. C. Chen | 27. | H. E. Trammell |
| 7 | N. Domingo | 28. | G. L. Yoder |
| 8. | D. M. Eissenberg | 29. | J. T. Cockburn (Consultant) |
| 9 | W. Fulkerson | 30. | R. E. Goodson (Consultant) |
| 10-14. | A. Golshani | 31. | T. J. Hanratty (Consultant) |
| 15. | H. W. Hoffman | 32. | T. R. LaPorte (Consultant) |
| 16. | L. Jung | 33. | L. F. Lischer (Consultant) |
| 17. | R. J. Kedl | 34. | R. N. Lyon (Consultant) |
| 18 | R. L. Linkous | 35. | D. J. Rose (Consultant) |
| 19 | J. F. Martin | 36. | V. K. Smith (Consultant) |
| 20 | J. W. Michel | 37 | ORNL Patent Office |
| 21. | R. W. Murphy | 38. | Central Research Library |
| 22. | M. Olszewski | 39. | Document Reference Section |
| 23. | S. A. Reed | 40-41. | Laboratory Records Department |
| 24. | R. C. Robertson | 42. | Laboratory Records, RC |
| 25. | T. W. Robinson, Jr. | | |

EXTERNAL DISTRIBUTION

43. S. Baron, Burns and Roe, Inc., 700 Kinderkamack Rd., Oradell, NJ 07649
44. E. S. Burcher, Branch Chief, Ocean Energy Systems Division, Department of Energy, 600 E. St., NW, Washington, DC 20585
45. A. F. Charwat, Dept. of Mechanics and Structures, University of California, 5731 Boelter Hall, Los Angeles, CA 90025
46. T. Fort, Department of Chemical Engineering, Carnegie-Mellon University, 500 Forbes Ave., Pittsburgh, PA 15213
47. S. Gronich, Branch Chief, Ocean Energy Systems Division, Department of Energy, 600 E. St., NW, Washington, DC 20585
48. W. Hahn, Office of Water Research and Technology, Department of Interior, Washington, DC 20240
49. F. Herbaty, Technology Management Branch, Chicago Operations and Regional Office, DOE, 9800 South Cass Ave., Argonne, IL 60439
50. D. H. Johnson, Solar Energy Research Institute, 1536 Cole Blvd., Golden, CO 80401
51. E. H. Kinelski, Program Manager, Ocean Energy Systems Division, Department of Energy, 600 E. St., NW, Washington, DC 20585
52. D. C. Kung, Technology Management Branch, Chicago Operations and Regional Office, DOE, 9800 South Cass Ave., Argonne, IL 60439
53. H. L. Liu, Hydronautics, Inc., Pindell School Rd., Laurel, MD 20810
54. J. J. McKetta, Dept. of Chemical Engineering, University of Texas, Austin, TX 78712
55. A. E. Molini, Chemical Engineering Dept., University of Puerto Rico, College Station, Mayagüez, Puerto Rico 00708

56. Larry I. Moss, P.O. Box 1496, Estes Park, CO 80517
57. T. R. Penney, Solar Energy Research Institute, 1536 Cole Blvd., Golden, CO 80401
58. T. Rabas, Westinghouse Electric Corp., Power Generation Divisions, Lester, PA
59. K. F. Read, U.S. Naval Academy, Annapolis, MD 21402
60. S. L. Ridgeway, R&D Associates, 4640 Admiralty Way, P.O. Box 9695, Marina del Rey, CA 90291
61. J. W. Rushing, DOE, Oak Ridge Operations, Oak Ridge, TN 37830
62. B. Shelpuk, Solar Energy Research Institute, 1536 Cole Blvd., Golden, CO 80401
63. L. A. Spielman, Dept. of Civil/Chemical Engineering, University of Delaware, Newark, DE 19711
64. L. J. Thibodeaux, Dept. of Chemical Engineering, University of Arkansas, Fayetteville, AR 72701
65. G. B. Wallis, School of Engineering, Dartmouth College, Hanover, NH 03755
66. L. Wechsler, Hydronautics, Inc., Pindell School Rd., Laurel, MD 20810
67. K. R. Weisbrod, Dept. of Chemical Engineering, The University of Illinois, Champaign, IL 61801
68. C. E. Wicks, Dept. of Chemical Engineering, Oregon State University, Corvallis, OR 97331
69. C. Zener, Dept. of Physics, Carnegie-Mellon University, 5000 Forbes Ave., Pittsburgh, PA 15213
70. Office of Assistant Manager for Energy Research and Development, DOE, ORO, Oak Ridge, TN 37830
- 71-331. Given distribution as shown in DOE/TIC-4500 under category UC-64 (Ocean Energy Systems)